PROCEEDINGS A

royalsocietypublishing.org/journal/rspa

Review

Cite this article: Mohanty S, Khalil ISM, Misra S. 2020 Contactless acoustic micro/nano manipulation: a paradigm for next generation applications in life sciences. *Proc. R. Soc. A* **476**: 20200621.
https://doi.org/10.1098/rspa.2020.0621

Received: 31 July 2020
Accepted: 20 October 2020

Subject Areas:
engineering

Keywords:
microrobotics, acoustic tweezers, acoustofluidics, lab-on-a-chip, self-propulsion, minimally invasive surgeries

Author for correspondence:
Sumit Mohanty
e-mail: s.mohanty@utwente.nl

Contactless acoustic micro/nano manipulation: a paradigm for next generation applications in life sciences

Sumit Mohanty[1], Islam S. M. Khalil[1] and Sarthak Misra[1,2]

[1]Surgical Robotics Laboratory, Department of Biomechanical Engineering, University of Twente, 7522 NB Enschede, The Netherlands
[2]Surgical Robotics Laboratory, Department of Biomedical Engineering, University Medical Center Groningen, 9713 AV Groningen, The Netherlands

SM, 0000-0002-7423-3611

Acoustic actuation techniques offer a promising tool for contactless manipulation of both synthetic and biological micro/nano agents that encompass different length scales. The traditional usage of sound waves has steadily progressed from mid-air manipulation of salt grains to sophisticated techniques that employ nanoparticle flow in microfluidic networks. State-of-the-art in microfabrication and instrumentation have further expanded the outreach of these actuation techniques to autonomous propulsion of micro-agents. In this review article, we provide a universal perspective of the known acoustic micromanipulation technologies in terms of their applications and governing physics. Hereby, we survey these technologies and classify them with regards to passive and active manipulation of agents. These manipulation methods account for both intelligent devices adept at dexterous non-contact handling of micro-agents, and acoustically induced mechanisms for self-propulsion of micro-robots. Moreover, owing to the clinical compliance of ultrasound, we provide future considerations of acoustic manipulation techniques to be fruitfully employed in biological applications that range from label-free drug testing to minimally invasive clinical interventions.

THE ROYAL SOCIETY PUBLISHING

1. Introduction

Non-contact manipulation methods form an integral part of modern-day microsystem technology and provide prospects for diverse biomedical applications from tissue engineering to clinical diagnostics. Many of these applications require the manipulation methods to achieve safe, low-power and precise handling of sensitive micro-agents such as cells, bio-molecules and bio-organisms [1]. In order to ascertain such low-power and reliable actuation, these manipulation methods judiciously harvest energy provided by indirect physical forces to enable locomotion of target micro-agents. Various physical mechanisms based on optics [2], magnetism [3], plasmonics [4] and acoustics [5] have been exploited for remote actuation of synthetic and biological agents. Optical tweezers have been the most primitive technology that employs focused laser beams to trap agents across a wide range of sizes (100 nm–1 mm) [2,6]. Besides the costly and complex optical hardware required in optical tweezers, the high-power operation of lasers may damage living or otherwise sensitive biological specimens. Plasmonic tweezers on the other hand, are low power variant of optical tweezers capable of much finer nanomanipulation. However, they require a nano-structured substrate to control light beams for high-resolution traps and also suffer from heat dissipation into the surrounding environment [1,4]. Magnetic tweezers are ubiquitous in DNA manipulation though they provide low resolution for video inspection via microscopy [7]. Moreover, the requirement for high magnetic field or gradient burdens the instrumentation of magnetic tweezers. These trade-offs necessitate a low-power actuation tool that offers a broad range of target size for micromanipulation.

Contactless actuation using acoustics has emerged as a low power, biocompatible and versatile technique that overcomes these aforementioned limitations of other manipulation methods [1,5,8–10]. The techniques employing acoustic manipulation exist in a broad operating frequency range of 100 Hz–100 MHz. Consequently, acoustic actuation techniques can manipulate agents across several orders of magnitude in size, from clusters of nanoparticles up to a millimetre-sized biological worms [5]. Furthermore, this frequency range complements the operating range of ultrasound imaging devices which makes acoustic manipulation techniques suitable for clinical applications. Importantly, most of the acoustic manipulation techniques use sound intensities of less than 10 W cm^{-2} on the target agents which makes them safe for sensitive label-free handling of biological agents such as embryos and cells [1].

In terms of versatility, acoustic manipulation techniques can be employed to trap and manoeuver particles as acoustic tweezers [11] or enable fast fluid transport to pump and mix different liquids [8]. Acoustic tweezers are devices that use focused sound waves to trap and manipulate agents. These are typically bulk acoustic wave (BAW) tweezers for three-dimensional (3-D) manipulation in air [12], and surface acoustic wave (SAW) tweezers for two-dimensional (2-D) manipulation in fluid [5]. In case of BAW tweezers, sound waves propagate through the bulk of a medium whereas for SAW tweezers, sound waves propagate along an elastic interface and decay into the surround medium, generally fluids. SAW devices extend from tweezers in confined fluidic reservoirs to devices for flow-assisted patterning of agents in microchannels [9]. Additionally, many acoustofluidic devices employ sound-fluid interaction to indirectly exert forces on target agents. These devices enable localized fluid oscillations to generate an induced flow for long-range transport of both fluid and agents [13]. Overall, the methods described here do not involve any active participation of the agent for their actuation. These technologies benefit from the intelligence, dexterity and efficiency of the actuation process, and the instrumentation behind it. We classify such technologies that function on off-board powering mechanisms as *passive* actuation techniques.

Various other remote actuation strategies exploit the self-propulsion ability of the agent triggered by their acoustic excitation to specific resonant frequencies [14–16]. These agents actively participate in their actuation process by means of an on-board powering unit that mobilizes them remotely. The most prolific of these are agents containing air-cavities or flagella that vibrate to generate localized fluid oscillations which leads to their directional propulsion [16,17]. Design and development of such agents is premised upon innovative microfabrication

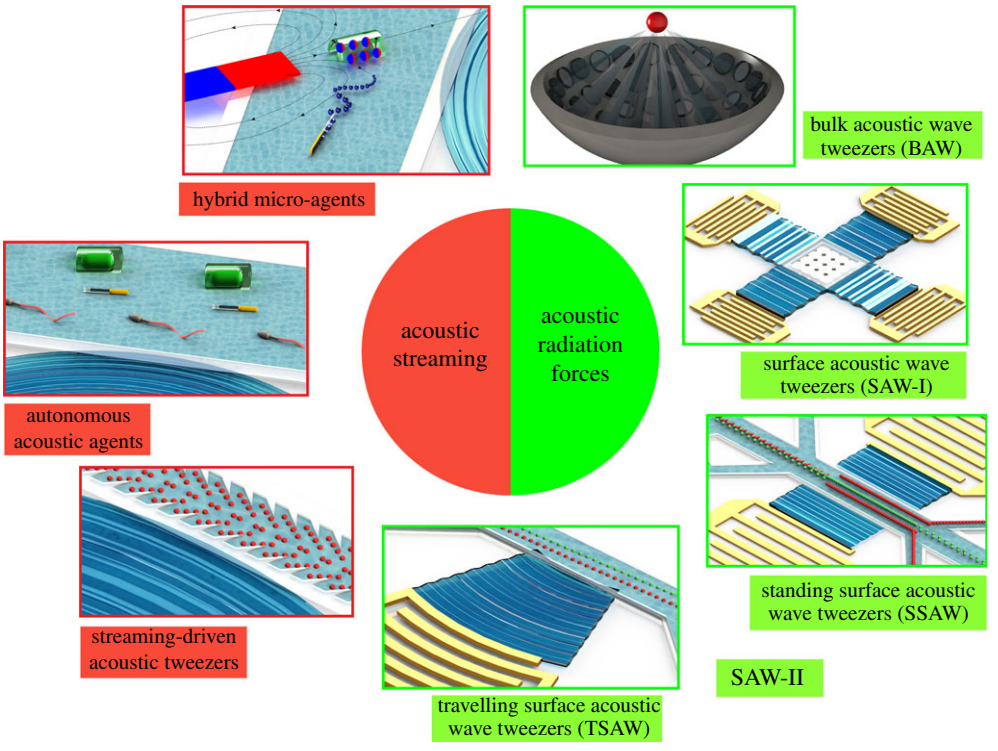

Figure 1. A schematic of acoustic manipulation techniques: Passive manipulation strategies that consist of various types of acoustic tweezers, and active manipulation strategies that employ autonomous and hybrid micro-agents. (Online version in colour.)

techniques, material composition or chemical functionalization of the agents post-synthesis. Such actuation strategies contribute towards microrobotic technologies that play a pivotal role in next generation surgical interventions [18,19]. Such technologies are classified here as *active* actuation techniques.

A gamut of previous literature surveys provide a comprehensive assessment of acoustic tweezers based on BAW [10,12], SAW [8,9,20] or both [1,5]. However, a few reports address acoustically actuated autonomous agents and are typically limited to only a single type of agent [15,21]. In this survey, we present a global perspective of the known methodologies in acoustic manipulation technology (figure 1). This survey is organized as follows. Firstly, we discuss the fundamental theory behind different actuation strategies in §2. In §§3 and 4, we cover the aforementioned passive and active actuation mechanisms, and their applications, respectively. Additionally, we describe hybrid actuation strategies in §4 where acoustic manipulation techniques work in tandem with other physical mechanisms, notably magnetic actuation. Thereafter, in §5, we provide our insight over improvements and future directions of the different actuation strategies for their prospective biomedical applications. Finally, we summarize the actuation strategies and our recommendations for their respective technologies that may advance the field of acoustic manipulation.

2. Acoustic forces acting on a target agent

The propagation of sound through air or liquid medium may generate forces on immersed or suspended agents, known as radiation forces. These forces arise due to the difference in the acoustic properties of the agents with respect to that of the medium [10]. Alternatively, sound

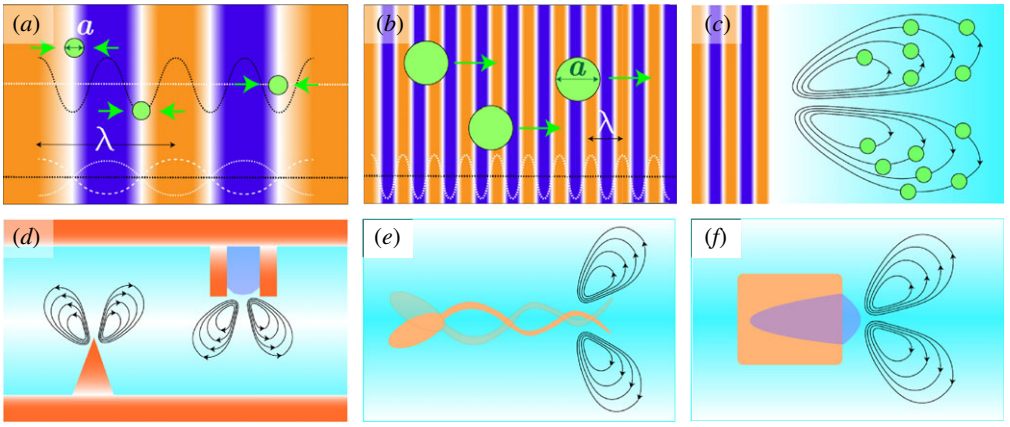

Figure 2. Acoustic radiation forces acting on agents of size (a) when exposed to sound waves of wavelength (λ) where, $k = 2\pi/\lambda$: (a) scenario $ka \ll 1$: gradient forces acting on agents under standing waves that results into a potential field, U; (b) scenario $ka > 1$: scattered forces acting on larger agents under travelling wave propagation; (c) scenario $ka < 1$: streaming induced drag forces acting on agents, (d) microchannel protrusions showing streaming patterns under vibration. Microstreaming effects around self-propelling agents under acoustic excitation: (e) asymmetrically designed flagellated microswimmer and (f) bubble-powered micro-propeller. (Online version in colour.)

waves may also put the surrounding medium into motion owing to a phenomena known as acoustic streaming, and thereby indirectly influence the agents present in the medium. Nearly, all the analytical models describing the acoustic radiation forces are premised upon the overall largest dimension (a) of the target agent, relative to the acoustic wavelength (λ) [5,9,11]. The general formulation of acoustic radiation force is derived from first-order acoustic pressure acting on the agents, that comprises of *gradient* and *scattered* forces. The *streaming* effects result from second-order acoustic pressure and nonlinearities in the governing sound–fluid interaction [22,23]. As a result, the streaming-induced forces act indirectly on the target agent owing to the localized oscillations in the surrounding fluid. Hence, the overall force on the agent can be described in terms of these components (denoted by respective subscripts) as

$$\mathbf{F}_{\text{total}} = \mathbf{F}_{\text{grad}} + \mathbf{F}_{\text{scatter}} + \mathbf{F}_{\text{stream}} \tag{2.1}$$

Hereon, the dominance of above-mentioned force contributions is discussed based on the relation between sound wavelength and size of the agent (figure 2). Specifically, the first term ($\mathbf{F}_{\text{grad}}$) in the right-hand side (r.h.s.) of (2.1) scales as ka^3, while the remaining terms in r.h.s. scale as ka^6 (where $k = 2\pi/\lambda$) [5,10]. Given this dependency, the gradient forces are dominant in Rayleigh regime ($ka \ll 1$), while the scattered forces are dominant in the Mie regime ($ka > 1$). The streaming-induced forces typically apply to agents when $ka < 1$ while their relative magnitude depends on the workspace dimensions [9,11].

(a) Radiation forces on target agents

When target agents are much smaller than the acoustic wavelength, they can be treated as compressible spheres of diameter (a) to propagating sound waves [10]. In this case, these agents can be manipulated with the application of gradient forces that can be described in terms of an acoustic potential field (U), as [24]:

$$\mathbf{F}_{\text{grad}} = -\nabla U,$$

$$\text{where } U = \frac{4\pi}{3}a^3\left[f_1\frac{1}{2}\kappa_o\langle|p_1|^2\rangle - f_2\frac{3}{4}\rho_o\langle|\mathbf{v}_1|^2\rangle\right],\ f_1 = 1 - \frac{\kappa_p}{\kappa_o} \text{ and } f_2 = \frac{2(\rho_p - \rho_o)}{2\rho_p + \rho_o}. \tag{2.2}$$

In (2.2), $\langle|p_1|^2\rangle$ and $\langle|\mathbf{v}_1|^2\rangle$ refer to the mean value of gradient pressure and particle velocity of the first order, over a time period of sound propagation, respectively. Furthermore, κ_* and ρ_* describe the compressibility and density for the agent ($*=p$) and the fluid medium ($*=o$), respectively. In (2.2), κ_o and ρ_o are related with the speed of sound c as $\kappa_o = 1/\rho_o c^2$. The gradient forces are prominent in case of standing waves where counter-propagating waves exert these forces on the agent from both the sides. As a result, the targeted agents can be trapped in pressure nodes of minimum potential (figure 2*a*). This strategy is capitalized in acoustic tweezers based on superimposition of two or more sound waves (§3a). Furthermore, the contrast in material properties of the agent determines its trapping position in a standing wave field. Case in point, the agents with $\rho_p > 0.4\rho_o$ move towards the pressure nodes of the standing wave field whereas those with $\rho_p < 0.4\rho_o$, navigate towards the pressure antinodes [5].

On other hand, for bigger size of target agent (i.e. $ka > 1$), the scattered component of radiation forces ($\mathbf{F}_{\text{scatter}}$) overcome the gradient forces ($\mathbf{F}_{\text{grad}}$) acting on it due to their higher-order dependency on size [10]. Importantly, many microfluidic tweezers (§3b) operate in this regime where agents can either absorb or reflect incoming sound waves (figure 2*b*). As a result, the travelling waves-based tweezers exploit scattered forces to provide a focused flow of target agents. For comparison, standing waves of kHz order can trap a target agent of 10 µm, while can be made to translate along travelling waves in MHz range.

(b) Streaming effects in microchannels

Besides the radiation forces, acoustic tweezers discussed previously also encounter streaming effects usually dominant near oscillating solid–fluid boundaries. Although as microfluidic workspaces typically have a high surface area compared to overall volume of fluid, streaming-driven forces operate well within the bulk of bounded medium. In several instances streaming-induced drag forces enable out-of-plane manoeuvering of agents for 2-D acoustic traps [25] and vibrating Chladni plates [26]. Fundamentally, acoustic streaming results from the viscous absorption of sound waves as they propagate from a vibrating solid boundary into the fluid medium [5,11,22,23]. As a result, the response of fluid to harmonic sound propagation yields a first-order component ($\mathbf{v}_1$) and a dominant second-order term ($\mathbf{v}_2$) among other higher order components. This second-order component manifests into counter-flowing fluid fluxes near the vibrating boundary that forms an overall steady flow over a periodic cycle of wave propagation i.e. $\langle\mathbf{v}_2\rangle$. The streaming forces originate from a Reynold's pressure of the form ($\rho_o\langle(\mathbf{v}_1.\nabla)\mathbf{v}_1\rangle$) and a second-order acoustic pressure field (p_2) acting on the fluid. These components arise from the governing acoustofluidics theory (based on Navier–Stokes and continuity equations) that can be simplified to represent acoustic transmission ($\mathbf{v}_1$) and resultant fluid flow ($\langle\mathbf{v}_2\rangle$) on different time scales [22,23]. Consequently, a boundary-driven streaming originates within a critical depth (δ_v), near the vibrating boundary which further gives rise to a bulk streaming in a bounded fluid channel. Given the dimension w of workspace in direction of sound propagation, the influence of boundary-driven streaming is pronounced when

$$\lambda \gg w \gg \delta_v. \tag{2.3}$$

In (2.3), $\delta_v = \sqrt{2\mu/\rho_o\omega}$, where μ is the viscosity and ω is the frequency of the sound wave. This resultant bulk streaming can induce acoustophoretic motion of agents at MHz range of frequencies (figure 2*c*). For this case, Muller *et al.* describes the regime where streaming forces dominate over scattered forces for agents below a critical size relative to workspace considerations (2.3) [22]. A comprehensive overview of various streaming phenomena and their respective regimes has been described by Wiklund *et al.* [11].

Typically, streaming-induced fluxes can locally capture and manoeuver agents in the vicinity of (δ_v). Although for microchannels with high aspect ratio, these fluxes can lead to a large circulation of agents in the bulk of the channel. This boundary-driven streaming can however be enhanced with the provision of various indented structures along the boundary such as sharp protrusions [23] or air-bubble pockets [27] (figure 2*d*). Vibration of these structures produce counter-flowing

vortices in their near field which results in a steady flow ($\langle \mathbf{v}_2 \rangle$) in the far-field of the channel. Application of this method involves design and modelling of these protruding structures on the boundaries of targeted workspace [23]. This strategy has been used for directional fluid flow and long-range transport of target agents (§3c).

(c) Streaming-induced forces on target agents

Going beyond workspace geometry, intentionally designing the agents with vibrational units can enable their autonomous propulsion based on streaming forces. These self-propelling agents comprise of either an asymmetric profile [14] or trapped air bubbles [16] that vibrate to acoustic frequencies to produce microstreaming around them (figure 2*e* and 2*f*). For such agents, the radiation forces are calculated by integrating the second-order pressure and a term analogous to Reynold's pressure, around a boundary enclosing the agent as

$$\mathbf{F} = -\left\langle \oint p_2 \mathbf{n} \, \mathrm{d}S \right\rangle - \left\langle \oint \rho_o (\mathbf{n}.\mathbf{v_1}) \mathbf{v_1} \, \mathrm{d}S \right\rangle, \tag{2.4}$$

where $\mathbf{n}$ is an outward normal to the surface of the agent and S defines the boundary enclosing the agent [10]. The first term in the r.h.s. of (2.4) describes the microstreaming component whereas the second term describes the vibrations induced in extended agents that can be remotely actuated as swimmers [28] (§4a). Autonomous agents with trapped air bubbles encounter radiation forces acting on the bubbles, known as Bjerknes forces, that translate them in the direction of sound propagation [29]. In their case, stable oscillations of bubble at high frequencies induce a microstreaming flow ($\langle \mathbf{v}_2 \rangle$) around them analogous to the case of extended swimmers [11]. Agents with one side of the bubble exposed to the fluid produce asymmetric microstreaming around them which imparts a propulsive force in the direction opposite to the flow [30]. These bubble-powered agents propel at their resonant frequencies (f_o) dependent on the predefined geometry of their air-filled cylindrical cavities, and can be expressed as

$$f_o = \frac{1}{2\pi} \left(\frac{\gamma P_o}{\rho_o (L - L_b) L_b} \right), \tag{2.5}$$

where P_o is the ambient pressure in the liquid, γ is the adiabatic index, L_b is the length of the trapped bubble and L is the total length of the cylindrical cavity [17]. Lastly, the sound scattered from nearby bubbles or particles can exert a secondary radiation force on the agent which enables them to carry other objects (§4b). Hereon, we investigate different acoustic manipulation strategies with regards to the aforementioned theory of radiation and streaming-induced forces.

3. Passive agents and actuation strategies

Passive actuation strategies comprise of off-board powering methods to energize the target agent that either remains inactive or does not contribute to their actuation process. These strategies either create pressure disturbances in the medium to trap the agents, or exert forces on them based their relative acoustic contrast to the medium. The target agents usually comprise of micro-particles, cells and biological specimens like Zebrafish embryos, pollen grains and immobilized *Caenorhabditis Elegans*. Since these agents lack the autonomy in their physical manipulation, the burden of manipulation entirely lies on the actuation system. Hence, we explore passive acoustic manipulation strategies where the innovation revolves around the following factors:

— Instrumentation, system integration and programmability of acoustic actuation units;
— Design and synthesis of the target workspace for manipulation;
— Numerical modelling of sound–fluid interactions occurring at interfaces.

Based on the role of the aforementioned factors in determining the actuation principle, we classify our manipulation strategies into three major areas. Firstly, we cover acoustic levitation or tweezing of micro-agents in a bounded medium based on BAW or SAW [31–52]. Here, we

divide SAW-based tweezers into two subcategories where we first discuss the devices that operate on static or enclosed reservoirs as the target workspace i.e. SAW-I devices [46–52]. Secondly, we delve into microfluidic SAW devices i.e. SAW-II, where an external flow in microchannels enables a flow-guided patterned segregation of different target agents [53–76]. Lastly, we discuss acoustofluidic devices called streaming-driven tweezers, where acoustically driven flow enables both fluid manipulation and transport of agents trapped in streaming-induced fluid oscillations [77–91].

(a) Acoustic tweezing in enclosed workspace

The most primitive idea to exploit acoustic energy for manipulation is to suspend particles [31] and droplets [34] above an acoustic transduction platform and manoeuver them as they levitate in the air. The principle of operation here is to apply gradient forces to trap the target agents in a bounded workspace, which can be both air and liquid medium. Given that gradients forces are dominant in Rayleigh regime, i.e. $ka \ll 1$, agents in the size range 1 µm–1 mm can be manipulated with systems operable at frequencies greater than 40 kHz. Based on the agent size and target application, the manipulation techniques can be broadly classified as BAW and SAW-I tweezing, respectively. Generally, BAW tweezers employ standing waves or focused travelling waves from multiple sound sources to levitate objects in air [35,36,41]. In addition, there exist BAW-based resonant fluid chambers where standing waves are used for bulk patterning of micro-agents [33]. SAW-I tweezers on the other hand, operate on bounded fluid reservoir whereby incoming sound waves are coupled from one or multiple sound sources into the fluid via a shared substrate [25,46–48]. In both techniques, the design and distribution of acoustic transducers play a crucial role to ascertain controlled manipulation of the target agents. BAW devices generally employ array of commercially available cm-scale piezoelectric transmitters [31], ceramic sheets [33] or metallic transducers [32,92] for long-range transport of mm-sized agents. SAW-I devices often require planar micromachined transducers synthesized using photolithography, and are aimed at tissue engineering and laboratory-on-a-chip applications [9]. The distribution of transducers varies from rectangular [25,31] to circular [40,42,50] morphology to trap particles at desired focal points like an optical lens. Owing to this functional similarity with optical tweezers, this class of manipulation devices are referred as acoustic tweezers [1,25,41].

Acoustic tweezers have been employed in numerous applications like crystallography [93], cell cultures [92], contactless micro-mixing of droplets [34] and bio-printing [25] to name a few. Hereon, we discuss acoustic tweezing methods employing BAW and SAW that are confined to manipulation of agents in a enclosed workspace, which consist of an air-filled space or a bounded fluid reservoir. We focus here on the requisite instrumentation in terms of different configurations of transducers and the desired pressure field available for manipulation.

(i) Bulk acoustic manipulation

BAW tweezers are devices that are designed to manipulate 100 µm–1 mm sized particles, typically in air, with the operating frequencies of the transducers in the range of 500 Hz–100 kHz [12,34], with the exception of BAW resonators that operate at MHz frequencies [33]. BAW tweezers hold the ability for long distance transport (up to 100a) and assembly of macro-scale payload using multi-transducer arrays [31,45]. The central idea with the instrumentation here is to develop reconfigurable devices that provide a dynamic 3-D pressure field with the ability for spatial modulation of acoustic trap. Such a dynamic field enables real-time spatial manoeuvering of acoustic traps based on frequency modulation [38], phase modulation [39] or a combination of both [41]. The most ubiquitous of these systems are the ultrasonic phased arrays which can levitate and manoeuvre trapped agents across different focal points by varying phase difference between the transducers [31,34,45]. In terms of their configuration, the transducer arrays can be single-sided or double-sided, with planar or spherical morphology of transducer distribution. The double-sided configuration is the most traditionally followed setup where a transducer and

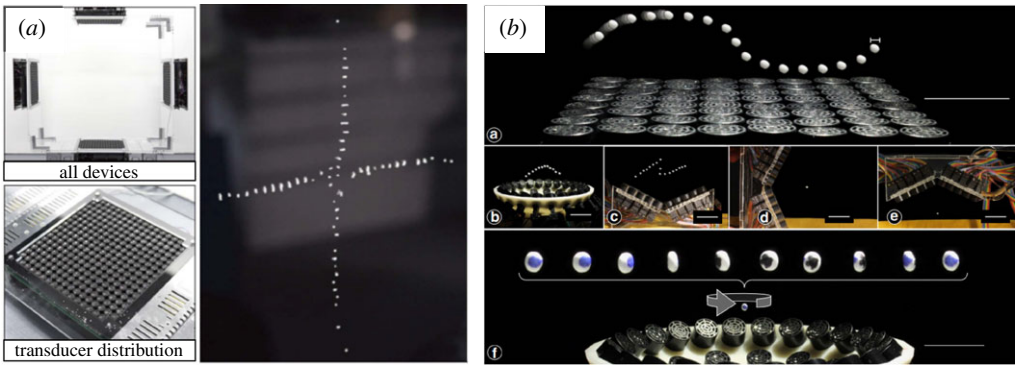

Figure 3. Different bulk acoustic manipulation methods: (*a*) two-sided configuration-based on planar arrangement of transducers (Adapted with permission from [31], © 2014 Ochiai *et al.* Licensed under CC BY 4.0.). (*b*) One-sided transducer configuration with planar and spherical arrangement of transducers (Adapted with permission from [41], © 2015 Marzo *et al.* Licensed under CC BY 4.0.). (Online version in colour.)

reflecting substrate [34,37] or mutually orthogonal transducers [31] form pressure nodes between them (figure 3*a*). On the other hand, the one-sided configuration typically consists of a planar, spherical or cylindrical arrangement of transducers [41] (figure 3*b*) and Bessel beam manipulators [40] with a focal point providing greater accessibility to the workspace. With the advent of rapid prototyping and fabrication techniques, the one-sided Bessel manipulators have matured into more intricately designed monolithic transducers that function as acoustic vortex traps [42] and holographic lenses [43].

The double-sided transducer configuration offers a confined volume which presents a bottleneck for the targeted specimen to fit in the limited available space for manipulation. Whereas the one-sided configuration has the advantage of a greater open volume for biomedical applications. Overcoming this limitation, a double-sided cylindrical array of transducers has been recently demonstrated as an end-effector of a robot to accomplish pick-and-place tasks opening possibilities for a mobile and remote actuation [45]. For both the configurations, the spherical morphology of transducer array offers a higher acoustic trapping force as compared to the planar array [35].

Furthermore, the optimization strategies for phase adjustments in mapping the acoustic fields led to the evolution of acoustic tweezers as holographic devices that offer additional degrees of manipulation [36,41]. With this speciality acoustic tweezers possess the ability to levitate, and orient multiple agents simultaneously. Similar to the working principle of their optical counterpart, the holographic acoustic tweezers offer a more promising future for biological applications as they provide higher radiation force while consuming less power [36].

(ii) Surface acoustic manipulation

SAW-I devices operate at a higher and more extensive frequency range compared to BAW devices i.e. 10 kHz to 50 MHz. Thus, they are able to create a finer grid of pressure nodes to trap agents down to nanoparticles. They comprise of planar pairs or array of transducers that typically enclose a bounded medium over a shared substrate. This bounded medium may comprise of a fluidic reservoir like PDMS microchannels [25,46–48,50], or simply a clamped metal substrate such as Chladni plate [26,52]. The most prevalent SAW-I devices are fluidic tweezers that are typically composed of a pair of inter-digital transducers (IDTs) deposited over a piezoelectric substrate like $LiNbO_3$ (figure 4*a*). Akin to BAW devices, SAW-I tweezers also exist as Bessel beam manipulators [47,50], and provide dynamic fields governed by phase or frequency modulation of different IDTs [46,48]. SAW-I tweezers are essential for microbiology and tissue engineering

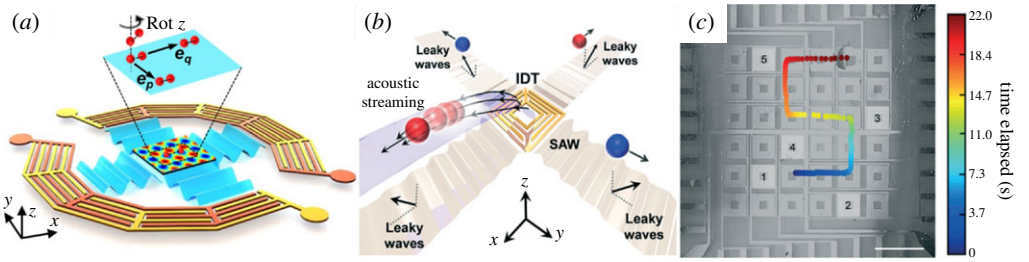

Figure 4. Different surface acoustic manipulation methods: (*a*) A surface acoustic tweezer based on a concentric network of miniaturized inter-digital transducers to generate micro-traps for particle manipulation. Here, reconfigurable acoustic traps can be produced by activating any two opposite pairs of inter-digital transducers. (Reproduced from [46]. © 2019 Tian *et al.*, some rights reserved; exclusive licensee American Association for the Advancement of Science. Licensed under CC BY 4.0.). (*b*) A programmable digital acoustofluidic pump for droplet manipulation. (*c*) Time-lapse trajectory assumed by a droplet upon selective actuation of inter-digital transducers. Scale bar is 5 mm. (Adapted from [48]. © 2019 Zhang *et al.* with permission from the Royal Society of Chemistry.). (Online version in colour.)

applications premised upon contactless handling of cell cultures [25,46,47] and fragile entities like embryos [48].

In addition to gradient forces, SAW-I tweezers also capitalize on streaming effects conditional to workspace geometry and acoustic wavelength as discussed earlier. For instance, micro-particles on a vibrating Chladni plate experience both in-plane acoustophoresis and an out-of-plane motion tendency owing to streaming-induced drag forces [26]. Interestingly, these out-of-plane streaming forces can levitate the target agents thus enabling 2-D tweezers to perform 3-D manipulation [25]. Furthermore, this phenomenon of streaming-induced acoustic traps have led to the development of digital acoustofluidic devices whereby a carrier droplet can be manoeuvered in a 2-D grid driven by hydrodynamic acoustic traps [48,51]. A variety of SAW-I tweezers for droplet manipulation has been discussed elsewhere [20].

Recently, more programmable configurations of SAW-I devices have been reported that enable precise path planning of target agents based on multiplexing actuators [46,48]. With advancements in photolithography, such a multi-nodal inter-digital transducer-based network has been demonstrated as an acoustofluidic micro-pump (figure 4*b* and 4*c*). As SAW devices overlap with microfluidic tweezers, we treat them as a separate sections where a continuous sheath flow in microchannels replenishes the target agents for manipulation.

(b) Microfluidic tweezers

SAW-II devices integrate microfluidic technologies with acoustic actuators where an external fluid flow enables continuous batch processing of micro-agents dissolved in solvents. These devices can be further classified into standing surface acoustic wave-based (SSAW) and travelling surface acoustic wave-based tweezers (TSAW) based on their ability to provide gradient ($ka \ll 1$) or scattered radiation forces ($ka > 1$), respectively. Similar in working principle to SAW-I devices, SSAW tweezers consist of double-sided IDTs enclosing a microchannel, bonded together on a substrate (figure 5*a*). Their operating frequencies are in the range of 100 kHz–100 MHz [53]. TSAW tweezers on the other hand, can operate with a one-sided IDT, usually with a curved morphology, adjacent to a microchannel (figure 5*b*) [54]. Their curved transducers provides the ability to focus sound waves on to a target agent as they propagate, and hence require a higher operational frequency of 100 MHz–1 GHz [55]. A detailed account of various IDT morphology and their functionalities is presented elsewhere [56]. The targeted applications of SAW-II devices include cell sorting [53,57–59], patterned tissue culturing [60], droplet microfluidics [61,62], separation of micro-particles from biological fluids [63–67], filtration of bio-organisms [68–72] to name a few.

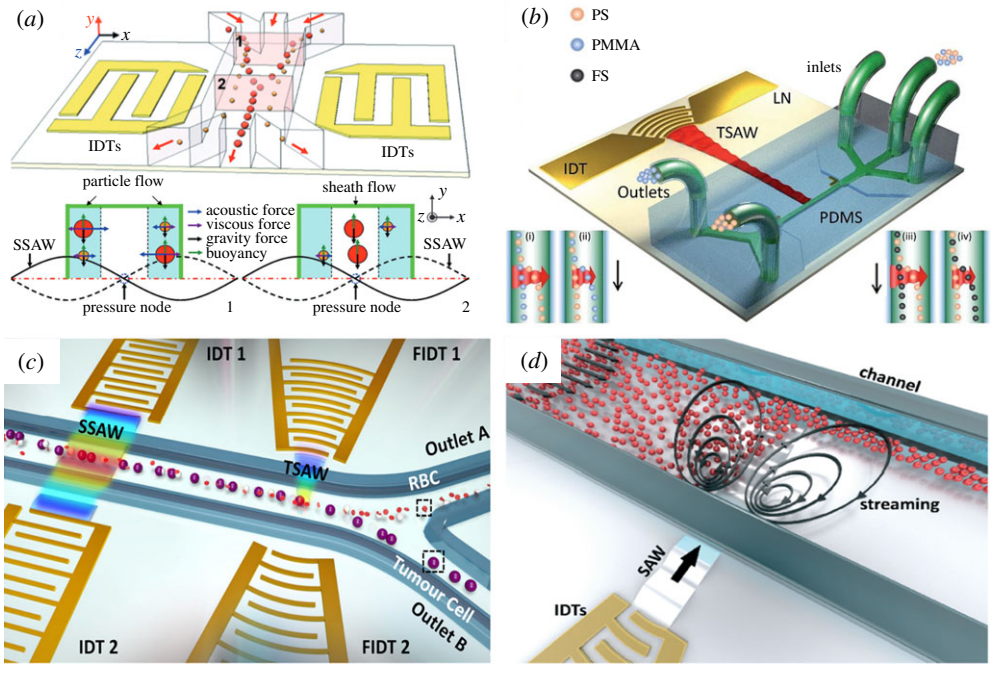

Figure 5. Different microfluidic tweezers based on (*a*) standing surface acoustic waves (SSAW) with a double-sided inter-digital transducers for micro-particle separation (Adapted from [53]. © 2009 Shi *et al.* with permission from the Royal Society of Chemistry.), (*b*) Travelling surface acoustic waves (TSAW) with a focused one-sided inter-digital transducers for separation of three different agents (Reproduced from [54] © 2017 Destgeeer *et al.* Published by the Royal Society of Chemistry.), and (*c*) A combination of standing surface acoustic wave (SSAW) and travelling surface acoustic wave (TSAW) tweezer with a double-sided configuration used for a two-step process of particle patterning followed by their separation Reproduced from [65] © 2017 Wang *et al.* with permission from Elsevier. SSAW operate via linear inter-digital transducers pairs whereas TSAW are generated using focused inter-digital transducers. (*d*) Combined application of acoustic streaming and radiation forces for focusing nanoparticles using one-sided curved inter-digital transducers Reproduced from [76] © 2017 Collins *et al.* Published by The Royal Society of Chemistry. (Online version in colour.)

The principle of operation for both SSAW and TSAW is premised upon the acoustic contrast of the target agents with respect to the fluid. Specifically, SSAW devices provide patterned segregation of agents based on differences in density in a multi-component fluid in the presence of a sheath flow [53,58,60]. Likewise, TSAW devices are employed as a more focused cell sorting technique in a sheathless manner, thus preventing any undesired dilution of the carrier fluid [59,73]. Additionally, TSAW devices have also been proven to be an effective tool to generate and channelize more compressible agents like droplets [62]. In comparison, SSAW devices possess excellent segregation ability while the TSAW devices provide a natural flow focusing ability to manipulate both the agents and the fluid [5]. Hence, various multi-stage SAW-II have been pursued as a two-step solution for high throughput agent segregation [59,66,74]. These SAW-II devices either consist of two stages each of SSAW [74] and TSAW tweezers [59], or a combination of both the device types (figure 5*c*).

In recent years, many SAW-II devices have been commercialized into industrial products like Ascent Bio-Nano^{TM} [70] and AcouSort^{TM} [66,71]. A commonly reported configuration of AcouSort^{TM} device enables segregation of bio-analytes from blood plasma in a multi-step fashion [66,67,71]. Recently, a variant of this aforementioned device has been reported that compensates for undesired streaming occurring in microchannels by optimizing its co-flow during the segregation [71]. On the other hand, various other SAW-II devices also capitalize on streaming effects [69,75,76]. They generate acoustically induced vortices for manipulation using

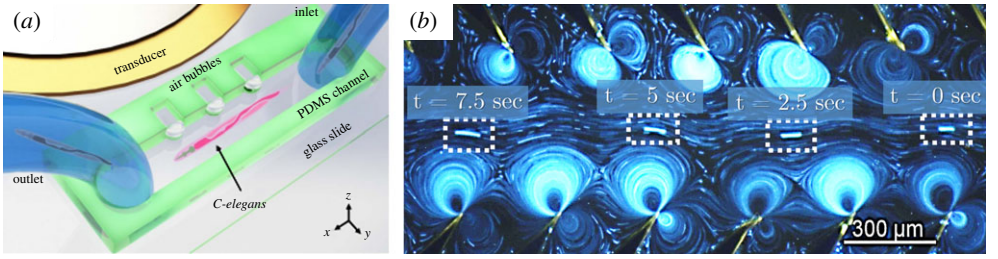

Figure 6. Different streaming-driven acoustic tweezers devices: (*a*) first generation streaming-driven devices that consists of microchannel workspace with symmetric air-filled side-wall cavities for micromanipulation of a *C. Elegans* worm. (Reproduced from [79] © 2016 Ahmed *et al.* with permission from Springer Nature. Licensed under CC BY 4.0.). (*b*) Second generation streaming-driven devices that consist of tilted protrusions for bi-directional transport of micro-agents (Reproduced from [88], © 2019 Mohanty *et al.* Licensed under CC BY 4.0.). (Online version in colour.)

focused IDTs (figure 5*d*). Next, we discuss acoustofluidic streaming-driven devices that explicitly generate streaming-induced vortices for flow-assisted micromanipulation.

(c) Streaming-driven acoustic tweezers

Many of the previously discussed devices harness streaming phenomenon as a secondary source of actuation for micromanipulation. Some prominent examples include droplet microfluidics [48], Chladni plates [26], focused TSAW tweezers [61,75,94] and acoustophoresis in microchannels [22]. Streaming-driven acoustofluidic tweezers are devices that are designed to exploit acoustic streaming to manipulate both the surrounding medium and agents immersed in it. These devices typically comprise of a microfluidic workspace with protruding vibrational structures on its boundaries, bonded on a shared substrate with a transducer. These vibrating structures produce the streaming-induced vortices that create an oscillatory fluid flow in bulk of the microchannels [23]. In contrast to SAW devices, streaming-driven tweezers rely on the workspace design more than that of the transducers. As a result, the scope of innovation in these devices shifts from sophisticated IDTs to construction of these specialized microchannels. Overall, these devices employ commercially available piezoelectric transducers that operate in the range of less than 100kHz to manipulate nm–µm size particles. Important applications of streaming-driven tweezers include transport of cells [77], pollen grains [80], manipulation of bio-organisms [78,79], micro-mixing [27,81], pumping [13,82–84] and enrichment of fluid mixtures [85,86].

The vibrational structures in streaming-driven devices comprise of either sharp protrusions [13,86–88] or air-filled cavities [79,80,83–85] indented at the boundaries of the microchannel. These structures can be incorporated in the bulk [27,81,89] or side-walls [78,79] of the channels to generate the requisite streaming effects. Broadly, streaming-driven devices exist in two major variants. The first generation of devices incorporate symmetric vibrational structures (figure 6*a*). These devices are primarily intended for localized mixing of fluids [27,86] or studying morphology of bio-species [78–80]. Here, the symmetrically indented structures to the microchannel walls provide counter-flowing vortices with no net directional flow in the channel. Whereas the second generation streaming-driven devices introduce an asymmetry in the design and distribution of vibrational structures to enable long-range transport of agents and fluids (6*b*). These devices contain tilted side-wall protrusions [13,87,88] and bubble columns [84,85] that offer a more directional fluid transport for micro-pumping applications. Furthermore, frequency-selective vibration of these tilted structures enable bi-directional steering of target agents inside these channels [83,88].

Recently, streaming-driven devices have incorporated long microfluidic trails as an extensive workspace [84–86], and use of active tethered components inside the channel for higher volumetric resolution [82,90]. Many of these devices have been synthesized with periodic cyclic

microchannel trails that facilitate multi-stage treatment of fluid samples for their enrichment [84,85] and purification [86]. On the other hand, a sophisticated assembly of IDTs within the workspace streaming-driven tweezers has been reported to achieve a pumping precision of nL s^{-1} [82]. In addition to these developments, streaming-driven devices have also been engineered with dynamic components such as acoustofluidic gears or rotors [89,91]. The fabrication strategy behind these acoustically powered gears later formed the basis for untethered micromachines based on acoustic streaming principles.

4. Active agents and actuation strategies

Previously described actuation methodologies apply on passive target agents that do not possess any autonomy for self-propulsion. Additionally, these passive agents lack the ability to cope with unpredictable conditions that are likely to be encountered in *in vivo* operations like fluctuations in pressure or fluid flow in their surrounding workspace. As a result, the collective burden of manipulation falls upon the accuracy of the actuation system and pre-existing knowledge of the workspace. This limitation makes the actuation process less compatible to *in vivo* studies and can be overcome with either designing agents with an on-board actuation unit or devising actuation strategy to be agent specific. Addressing such concerns, this section describes autonomous propulsion of active micro-agents, namely

— Self-propelling micro-agents based on standalone acoustic vibratory units [95–108].
— Hybrid acoustic micro-agents that function in tandem with magnetic and chemical actuation units [109–123].

The challenges associated with actuating these micro-agents shift from instrumentation and workspace design, towards synthesis and functionalization of the agents. Specifically, the photolithography techniques used in synthesis of IDTs mentioned earlier, have now been capitalized to design and develop multi-component artificial agents. Hereon, we survey different designs of active micro-agents with focus on their fabrication process and propulsion mechanism.

(a) Self-propelling acoustic micro-agents

Self-propelling micro-agents are specifically designed with geometrical shapes to enable their acoustic steering or functional units that vibrate to assist their locomotion. These micro-agents exist in diverse size and morphology, from nm-sized cylindrical rods to millimetre-sized assembly of vibratory micro-cavities. We classify these agents based on the underlying physical mechanisms, a majority of which are based on the streaming-induced forces (figure 2*e* and 2*f*). Specifically, they comprise of metallic nanorods [95–103], flagellated microswimmers [14,28,104] and bubble-powered micro-propellers [16,17,105–108,124]. Generally, these agents are actuated using commercially available piezoelectric transducers attached to a shared substrate that leaks sound waves into the medium in which they are immersed. Herein, we first describe the nanorods that rely partly on MHz range passive acoustic trapping while their directional self-propulsion is aided by their shape anisotropy. Thereafter, we subsequently delve into the other two micro-agents that contain self-actuating vibratory components tunable to kHz range frequencies.

(i) Metallic micro and nanorods

One of the first self-propelling agents capitalized on autonomous motion of axis-symmetric metallic micro- and nano-rods while they are acoustically levitated [95–101]. These micro-agents are made up of a single [96] or two dissimilar metals [95,97]. The actuation strategy applied here traps these nanorods in a nodal plane, while the in-plane acoustic streaming effects contribute to their propulsion [102,103]. The in-plane forces acting on these nanorods, arise owing to a heterogeneity in their profile, either in terms of density of materials [95,97] or shape anisotropy

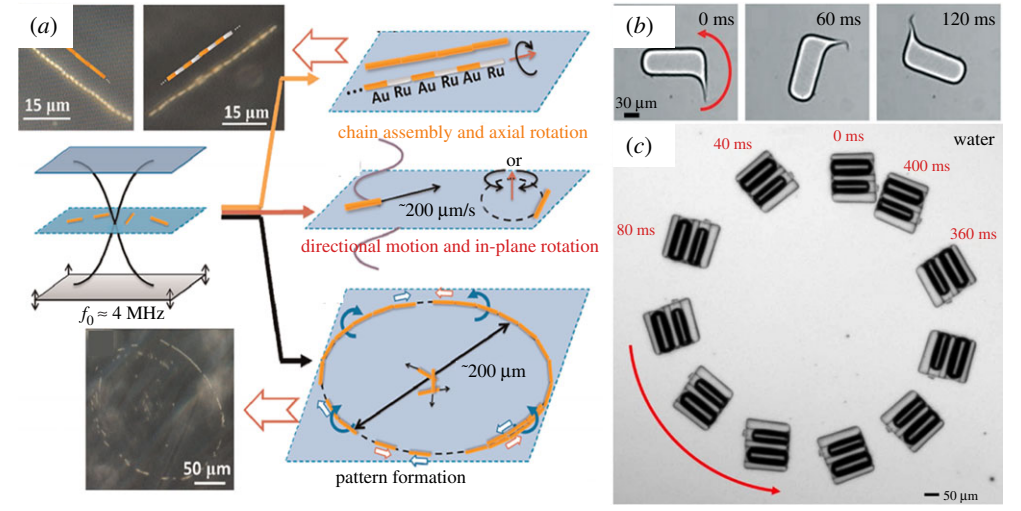

Figure 7. Different kinds of self-propelling acoustic micro-agents: (*a*) Acoustically trapped metallic nanorods undergo dynamic self-organization (Adapted from [95] © 2012 Wang *et al.* with permission from American Chemical Society.). (*b*) Rotational motion of a flagellated microswimmer (*marked by red arrow*) in response to sound waves (Reproduced from [14] © 2017 Kaynak *et al.* Published by the Royal Society of Chemistry.). (*c*) Rotational motion of a bubble-powered micro-propeller showing two bubble columns (Reproduced from [16] © 2015 Ahmed *et al.* with permission from Springer Nature. Licensed under CC BY 4.0.). (Online version in colour.)

[97,98]. Furthermore, the secondary forces acting on these rods can also enable their dynamic self-organization in linear or circular arrangements [95] (figure 7*a*).

These micro-agents are synthesized using template-based electrodeposition as cylindrically grown rods. Following their synthesis, they can be loaded with enzymes [100], proteins [99], cells [101] and dyes [99,101], which also enables their real-time fluorescent monitoring. Owing to this complimentarity with funtionalization, nanorods have found a gamut of biomedical applications like intra-cellular delivery [96,100], micro-RNA sensing [99] and toxin removal in blood samples [101]. Despite their promising *in vivo* applications, metallic nanorods often require them to be accurately positioned at the standing wave nodes. This poses difficulty for the nanorods to be employed in *in vivo* studies as they are less autonomous compared to other active micro-agents.

(ii) Flagellar acoustic microswimmers

Flagellar microswimmers have been designed to reciprocate the streaming effects of indented protrusions like in the case of streaming-driven tweezers. These swimmers comprise of an acoustically resonant flagellum that mimicks the flagellar dynamics of various biological and magnetic microswimmers during their motion [104]. In addition to acoustic streaming, the propulsion mechanism for these swimmers relies on induced structural vibrations in their flagella in response to incoming sound waves. These vibrations are attributed by the heterogeneous construction of the swimmers, which further amplify the microstreaming effects around the tip of their flagella [28]. Akin to metallic nanorods, the heterogeneity in these agents can be introduced with dissimilar material composition [28] or asymmetric shape of the flagellum [14]. These microswimmers can be synthesized using electrodeposition [28] or traditional UV lithography [14]. Several design variants of the aforementioned swimmers have shown their steerability (figure 7*b*) [14]. However, a single acoustic microswimmer capable of both translation and rotation is yet to be realized. Moreover, as these swimmers rely on effective coupling of surface acoustic waves to induce structural vibrations, their applications have been limited to microchannels.

(iii) Bubble-powered micro-propellers

Similar to vibrating protrusions, the microstreaming effects around oscillating bubbles described in §2, have been exploited to design self-propelling agents [16]. In this case, the micro-agents are powered by bubble-trapped columns, which are designed as open cavities of predetermined geometry, that resonate to specific acoustic frequencies. Analogous to flagellar acoustic swimmers, the shape asymmetry in terms of the position and size of cavity in these micro-propeller attributes to steering capability [16,105]. Additionally, actuation of bubble-powered micro-propellers can be selective to multiple frequencies owing to the presence of multiple cavities. As a result, the bubble-powered propellers can effectively perform both translation and rotational motion [105,106] (figure 7*c*). Alternatively, some instances of bubble-based propellers have been steered with the application of radiation forces using focused ultrasound transducers [124].

The traditional protocol for synthesis of acoustic micro-propellers consists of a standard 2-D photolithography followed by their development to obtain the micro-agents of a predefined cavity size [16,105,106,124]. This is followed by the surface treatment of agents to nucleate air bubbles inside their cavities once they are immersed in the fluid for operation. With the development of maskless 3-D nanoprinting, more complex and intricate geometries in the propeller designs have been reported [124]. Subsequently, larger prototypes of propellers came into existence with multiple micromachined cavities that offer higher degrees of mobility [106–108]. As these large propellers could be driven at kHz frequencies (refer (2.5)), they can be visualized using medical ultrasound (US) systems that operate at MHz frequencies. Recently, one such propeller has been reported to be both acoustically actuated and tracked under ultrasound guidance [106].

While many bubble-based propellers have achieved frequency selective steering, standalone acoustic actuation does not always provide adequate frequency range for both translation and rotation. Despite a large variance in bubble column length in many such propellers, only a narrow range of distinctly operable acoustic frequencies are achieved [105,106]. This calls for hybrid actuation approaches that enable independent directional control for these propellers, as will be discussion in the next section.

(b) Hybrid actuation strategies

Various hybrid actuation strategies combine acoustics with other physical mechanisms to impart directional navigation to the agents or control multiple agents while they are acoustically energized. In this category, we discuss strategies where acoustic manipulation has been applied in tandem with two commonly employed mechanisms namely, magnetic [109–118] and chemical [15,119–123] means of actuation.

(i) Magneto-acoustic actuation

Magnetic actuation has been the most ubiquitously employed technique for contactless manipulation across a wide size range of target agents. Likewise, acoustic manipulation methods under magnetic guidance find diverse strategies like assembly of magnetic agents [109], self-propelling acoustic agents [110–116], bio-hybrid agents [117] and collective behaviour of micro-particles [118]. The principle of actuation in all these strategies employs acoustic forces primarily to either levitate or propel the agents in the presence of an applied magnetic field. With regards to levitation, a BAW tweezer has been combined with a Helmholtz magnetic coil set-up to demonstrate multi-component assembly of mm-sized objects and droplets [109]. This combined actuation set-up (8*a*), supplies radiation forces to levitate magnetic agents, which can also orient themselves under magnetic guidance. Furthermore, the previously discussed self-propelling agents like metallic nanorods [110–112] and bubble-powered micro-propellers [113–116] have been re-engineered to accommodate magnetic components during their synthesis. In the former case, tri-metallic nanorods [110,111] and nanoshells [112] have been developed which use

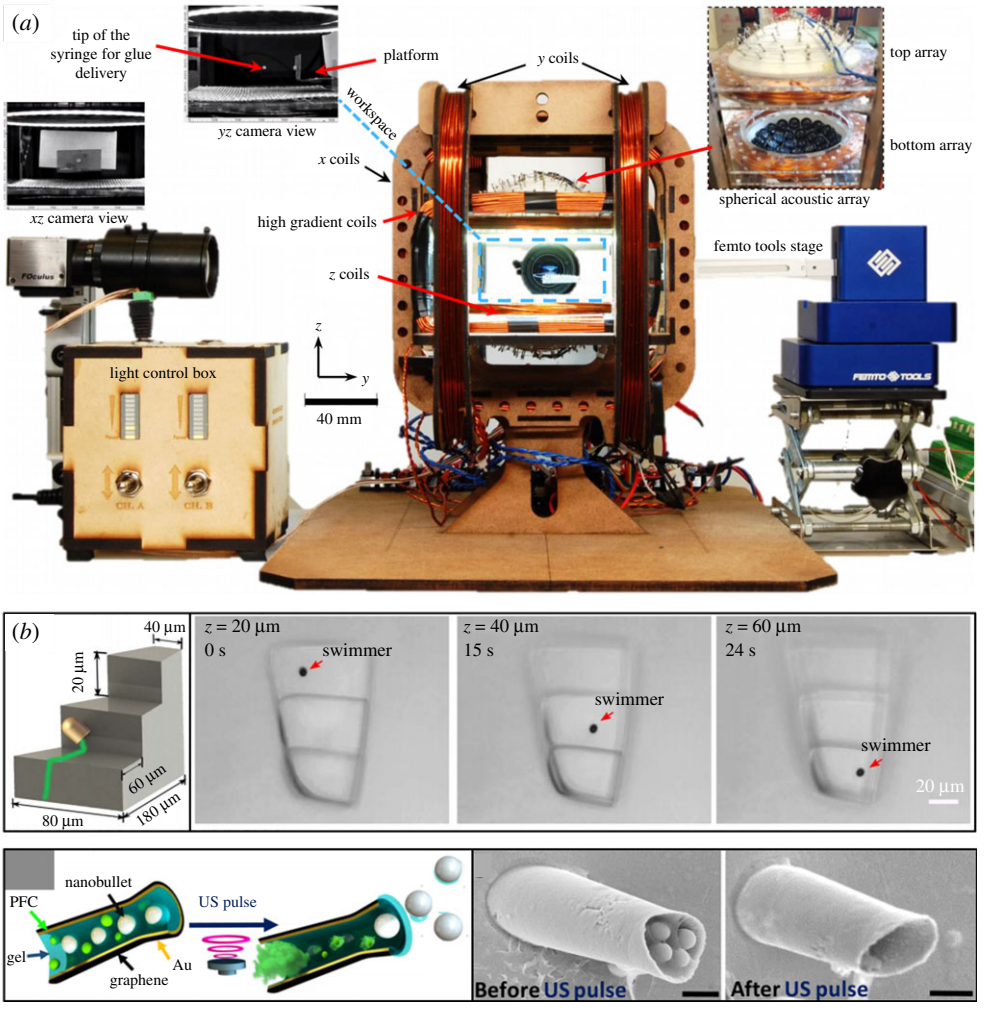

Figure 8. Different magneto- and chemo-acoustic hybrid actuation strategies: (*a*) Combined configuration of Helmholtz coils with ultrasound phased array for magnetically guided acoustic tweezing. The set-up shows various components that enables closed loop assembly of magnetic agents (Adapted from [109] © 2019 Youssefi *et al.* with permission from IEEE.). (*b*) Bubble-powered magneto-acoustic propellers with the ability to climb a 3-D nano-printed staircase (Image permission pending from Ren *et al.* [114] (Adapted from [114]. © 2019 Ren *et al.*, some rights reserved; exclusive licensee American Association for the Advancement of Science. Licensed under CC BY 4.0.). (*c*) Ultrasound triggered vaporization of encapsulated fuel enabling a ballistic microcannon. Scale bar is 20 µm. (Adapted from [120] © 2016 Soto *et al.* with permission from American Chemical Society.). (Online version in colour.)

the streaming due to their anisotropic profile along with magnetic guidance for directional motion. While on the other hand, the bubble-powered magneto-acoustic propellers evolved to provide advanced modes of locomotion aided by magnetic steering [113–116]. Specifically, they have been demonstrated to navigate complex trajectories [113] and climb along surfaces [114,115] with promising potential for bulk actuation (figure 8*b*). In addition, they can also perform pick-and-place operations capitalizing the secondary radiation forces to trap and eject particles [114].

In terms of biological applications, many of the magneto-acoustic micro-agents have been used for transport of cells [111,114], bacteria [110] and drug delivery to cancerous cells [112]. An interesting bio-hybrid actuation strategy involves functionalized magnetic Red Blood Cells, that can navigate through various biological media in the presence of both magnetic and acoustic

fields [117]. Another bioinspired approach mimicks collective behaviour of neutrophil cells in form of micro-particles that agglomerate under magnetic field, and can be manoeuvered in vasculatures aided by streaming effects [118]. When the magnetic field is switched off, this magnetically triggered formation can disembark to release an encapsulated drug at the target site. Recently, a bubble-powered multi-cavity propeller has also shown its ability for targeted drug delivery under combined magneto-acoustic guidance. Aside from the bubble columns for acoustic propulsion, this propeller also consists of a drug-filled cavity that can be triggered to release its contents at specific frequencies [116].

(ii) Chemo-acoustic actuation

Many prevalent strategies of chemotaxis have been combined with acoustics either as a triggering mechanism for propulsion [119,120], or a guiding force for navigation and organization of agents [121–123]. The first technique utilizes acoustic excitation of agents to catalyse ejection of chemical fuel as a microscale ballistic tool [119,120]. In this strategy, the agents are synthesized with an encapsulated emulsion that vaporizes on application of focused ultrasound pulse and releases the carrier particles (figure 8*c*). Whereas the second technique utilizes the acoustic self-propulsion of metallic nanorods, to achieve bi-directional motion induced by their chemical reaction in the surrounding medium [121,123]. The nanorods used in this approach act as catalyst to the surrounding fluid, whereby their chemical reaction yields an electro-osmotic flow which moves them forward [123]. Alternatively, the self-propulsion of chemical nanorods has been demonstrated with reversible swarm control triggered by acoustic radiation forces [122]. A more detailed account of chemically fueled acoustic agents has been reported previously [15]. However, limited clinical applications of chemo-acoustic agents exist as their dependence on a chemical medium or fuel does not allow their invasive operation.

5. Future considerations on emerging technologies

So far we have surveyed different contactless acoustic actuation strategies and described the recent advances in the state-of-the-art techniques. The importance of acoustic micromanipulation in life sciences can be deciphered from its versatile applications in biology and medicine. These technologies have the potential to serve as lab-on-chip based diagnostic platforms, and to be used for minimally invasive targeted interventions. With their dual advantage of both particle and fluid manipulation, acoustic tweezers exhibit diverse configurations for label-free handling of both sensitive biological agents and solvents. Acoustically triggered self-propulsion of agents provide autonomous means of actuation, thus paving way for targeted microrobotic applications. Although specific to their application, both passive and active actuation technologies can be vastly enhanced to extend their outreach towards translational clinical studies [1,5,12,21]. Firstly, acoustic tweezers have limited ability to transmit acoustic forces across tissues and in heterogeneous media like the blood plasma. In addition, while a majority of tweezers can accurately deploy multiple agents at their desired location, they seldom have the ability to trigger any functional response from the agents. These limitations necessitate improvements in the instrumentation and application strategy of tweezers. Acoustic tweezers can be employed with specialized agents which can be both manoeuvered to a target site, and triggered to carry out additional functions such as drug delivery and diagnosis. Furthermore, the tweezers may also act on autonomous agents and deploy them closer to the target site from where they can self-propel more reliably. On the other hand, while actuation of autonomous agents offers intelligent and agent-selective strategies, their standalone operation is less effective. Therefore, the collective action and 3-D actuation of these agents are desirable for targeted drug delivery. Besides these factors, visualization of these micro-agents under *in vivo* conditions calls for clinically compliant imaging techniques, most notably medical USA. In this section, we evaluate the aforementioned criteria and propose research directions that could precipitate additional innovations in the existing technologies.

(a) Instrumentation and operational efficacy of tweezers

Among acoustic tweezers, BAW devices are typically air-borne systems that manipulate larger agents (mm-scale) compared to SAW devices that operate on micro-particles mostly in fluids. BAW tweezers offer tremendous scope for integration with robotic platforms for navigation and visualization of agents across a large workspace [45]. Single-sided BAW tweezers may be interfaced to a programmable robotic [45] or haptic assembly [125] and manoeuvered around a surgical site to perform targeted operations. Furthermore, the instrumentation of BAW tweezers has evolved from static devices to holographic transducer elements for generation of dynamic high-resolution acoustic traps. Besides the miniaturization of transducers, research directions on use of holographic spatial sound modulators (SSM) can substantially enhance resolution of acoustic traps [126,127]. This technology holds the potential for simultaneous amplitude and phase modulation of acoustic beams using masks with sub-wavelength features.

On the other hand, performance of SAW tweezers depends on the design of IDTs and their ability to couple acoustic energy via piezoelectric substrates. The methods of generating surface acoustic traps have evolved to their phase- and amplitude- controlled re-configurable distributions using multiple concentric IDTs [46]. In this regard, a prospective research direction capitalizes on deep learning methods to generate spatially non-uniform acoustic field distribution for any given workspace design [128]. These approaches broaden the scope for SAW devices to manipulate target agents in dynamic patterns conformable to non-conventional microchannel geometries. Importantly, miniaturization and integration of SAW devices with flexible substrates and electronics can vastly extend their outreach towards *in vitro* applications [125]. In several instances, SAW technologies have been translated to wearable electrodes that enables deep penetration of acoustic waves to impact neurological studies in animal trials [129].

(b) Design and functionalization of autonomous agents

In case of autonomous agents, the reliable operation and ability to carry payload play a major role for their successful deployment in biological applications. Among these agents, bubble-powered propellers became popular due to their ease of actuation and convenient fabrication protocol. These micro-agents gained a huge impetus due to the developments in 3-D nanoprinting technology which led to a wave of eclectic propeller designs [106,114,124]. The next generation of these micro-propellers may consist of larger arrays of acoustically resonant cavities that can offer multiple degrees-of-motion. Alternatively, a different process flow can be pursued to achieve batch fabrication of much smaller nano-propellers that are equally adept at multi-modal locomotion [130]. Furthermore, in order to overcome bubble instability due to high-frequency oscillations, innovative measures are required in both the design and surface treatment of the propeller cavities. In this regard, secondary structures in the propeller designs can contribute additional surface tension at the bubble interface and impart longevity to their operation [115].

Aside from their synthesis, micro-agents can be functionalized to carry and release drugs or other agents for targeted therapy. In this regard, hybrid actuation strategies can play a crucial role for otherwise non-functional biological agents, as their acoustophoretic motion can be more directional under magnetic or chemical guidance [131]. Various chemo- and bio-functionalized metallic nanorods have been pursued for localized delivery of cells, drugs and RNA strands. Similar functionalities can be attributed to bubble-powered propellers, which can also use secondary radiation forces to carry and release a much heavier payload [114,130]. In addition to microstreaming around bubble columns, other alternative means to harvest acoustic forces on bubbles may be exploited as drug release or actuation mechanisms. Firstly, vaporization of carrier droplets triggered by pulsed ultrasound can serve as a method to release drugs encapsulated inside the propellers [116,132]. Secondly, mimicking US contrast agents, non-spherical modes of bubble oscillations may be exploited to facilitate directional release of drugs coated on the bubble interface of these propellers [133]. Although various such drug-coated micro-agents have been

standalone tested in 2-D microchannels, their limited ability to navigate 3-D workspaces impedes their progress towards *in vitro* clinical trials.

(c) Three-dimensional micromanipulation of target agents

Various clinical scenarios require the actuated agents to manoeuver through obstacles, cluttered environments and uneven surfaces like arteries which demand their 3-D manipulation. Primarily, BAW tweezers are the only qualified tools that are explicitly designed for bulk actuation of agents. Although SAW tweezers rely on surface transmission of acoustic energy, they can be smartly adapted to perform 3-D or upstream actuation of agents against gravity. Conventional SAW-based strategies may incorporate a more realistic workspace architecture that emulate tubular biological vasculatures [134,135]. A previously suggested method of designing flexible transducers or piezoelectric substrate may allow SAW devices to be attached to these tubular microchannels [125]. Moreover, next generation of streaming-driven tweezers may be envisioned with 3-D topographical features that allow streaming-induced migration of agents along sophisticated contours that imitate side-walls of blood capillaries [136]. Similar to passive agents, many autonomous propellers have been shown to ascend obstacles and curved surfaces. However, in most cases their 3-D actuation of agents is partly aided by hybrid actuation strategies [114,115,130]. A majority of the reported strategies of self-propulsion show minimal dependency on instrumentation. This leaves enormous scope for collaborative studies employing acoustic tweezers for more controlled two-step actuation of autonomous agents. In this regard, these agents can be initially steered to deep-seated locations in artificial phantoms or tissues using focused acoustic beams [133]. Thereafter, the agents can exploit their self-propulsion to reach nearby targets in an overall semi-autonomous fashion.

(d) Ultrasound-based imaging of micro-agents

Another important aspect imperative to clinical application is imaging of these agents in environments opaque to camera-based vision. Most of the actuation strategies reported so far are limited to traditional microscopy and are less suitable for non-invasive studies. With prospects of homogeneous actuation and surveillance, US imaging (MHz-GHz range) offers a suitable alternative for tracking micro- and nano-agents. The transducer arrays in BAW tweezers can be combined with commercially available US imaging probes for synchronized actuation and imaging of agents in biological tissues [137]. We envision the next generation of BAW devices to inherit features of US probes in order to transmit steerable acoustic beams inside the human body. Moreover, employing such specialized US probes on shared basis for actuation and tracking agents can open up opportunities for closed-loop studies in biological specimens. Alternatively, some of the reported technologies used for BAW tweezers may also serve as imaging elements for acoustic holographic displays [127,138]. Among autonomous agents, acoustic micro-propellers complement USA as coated gas bubbles are already in practice as contrast agents. In this context, these bubble-powered propellers may be designed to resonate at acoustic frequencies non-interfering with that required for US imaging. As a result, synchronized use of imaging probes and actuators can also be employed here to achieve ultrasound guided closed-loop servoing of these agents. However, the challenges that undermine US-based servoing of micro-agents is the resolution limit of the imaging probes. Although US probes (GHz range) may even detect up to nanoparticles in a noise-free environment, the tracking accuracy is noise-prone and thus compromised during a real-time clinical operation. One of the ways to overcome this limitation is to deploy groups of multiple agents that can easily be detected as a collective entity.

(e) Multi-agent manipulation

Collective actuation of multiple agents can boost the throughput in clinical applications compared to their standalone operation. It offers many advantages such as higher therapeutic dosage and

convenient clinical detection. With the ability to handle multiple agents, various acoustic tweezers can pattern or segregate agents with different acoustic properties. Yet many of these tweezers either cannot differentiate between similar agents, or are unable trigger a coordinated response from a specific type of agents. Here, advanced control strategies like iterative algorithms [36] and reinforcement learning [52] can be useful for agent-selective actuation. Nonetheless, the absence of external stimulus from the participating agents can make these advanced strategies less effective. Consequently, the passive collective actuation techniques may either lead to an over-actuated hardware or demand high computational power. Again, this provides opportunity for tweezers to collaborate with autonomous agents for a more controlled collective manipulation. Several instances of metallic nanorods and magnetic nanoparticles have shown swarming ability when triggered by USA. More interesting strategies for swarm manipulation may be devised based on secondary acoustic forces acting on bubble-powered propellers. Specifically, a single propeller can potentially capitalize on secondary radiation forces to attract or repel multiple neighbouring agents [130]. Prospective mechanisms may involve large formation of agents based on these secondary forces, that can be further manoeuvered as a swarm using other hybrid mechanisms [135]. Emerging strategies may extend to well-characterized agent–agent interactions that enable complex formations of autonomous micro-agents. Such dynamic formations might mimick the state-of-the-art magnetic swarms that can organize themselves as clusters and disembark into isolated agents upon removal of acoustic forces [139].

6. Conclusion

Our survey presents a panoramic view of acoustic micromanipulation methods targeting agents that range from mm-size size bio-organisms, microrobots and up to nanoparticles. Herein, we entail an eclectic set of devices that enable sound waves to trap these agents or transport them along microchannels, and different autonomous agents with self-propulsion ability. This report describes the governing physics, instrumentation, design, synthesis and control aspects for both the actuation platform and the target micro-agents. We finally aim to promote greater utility of acoustics in life science applications and stimulate collaborative research across different biomedical technologies premised on acoustic actuation.

We envision acoustic tweezers as diagnostic equipment, and self-propelling agents as microrobotic tools for prospective clinical applications. Notably, BAW tweezers are adept at automated manipulation and offer tremendous scope for integration with conventional robotic or haptic platforms. On the other hand, SAW tweezers provide a much higher resolution for localization and are important for cell patterning and tissue cultures. Various SAW devices have the potential to be commercialized into flexible diagnostic platforms that may be transformed into wearable devices. A collaboration between different SAW and streaming-driven tweezers can push the boundaries of their traditional usage in microfluidics, to design of acoustically driven surgical devices [140]. Lastly, we discuss self-propelling micro-agents with on-board vibrational units designed to resonate at specific acoustic frequencies. Besides their acoustic propulsion, these agents can join forces with other physical mechanisms like magnetism to allow for hybrid actuation. Offering prospects of swarm control and detection under medical USA, these agents are a promising tool for minimally invasive interventions. Nevertheless, the full potential of clinically relevant micro-agents has not yet been realized with combined studies on acoustic actuation and imaging of these agents under *in vivo* conditions. A futuristic surgical suite may combine several of these techniques, where autonomous micro-agents are deployed through a lumen using a streaming-driven tweezers at the target site while their swarms are manoeuvered using BAW tweezers.

Data accessibility. This article has no additional data.

Authors' contributions. S.Mo. conducted the research. I.S.M.K. and S.Mi. supervised the manuscript preparation. S.Mo. performed the survey and prepared the manuscript I.S.M.K. participated in the preparation of the manuscript and provided his guidance S.Mi. supervised the overall preparation of the manuscript.

Competing interests. We declare we have no competing interests.

Funding. This work was supported by funds from The Netherlands Organization for Scientific Research (Innovational Research Incentives Scheme-VIDI: SAMURAI project no. 14855).

Acknowledgements. The authors thank Dr Alvaro Marin for his suggestions in the preparation of the manuscript.

References

1. Ozcelik A, Rufo J, Guo F, Gu Y, Li P, Lata J, Huang TJ. 2018 Acoustic tweezers for the life sciences. *Nat. Methods* **15**, 1021–1028. (doi:10.1038/s41592-018-0222-9)
2. Ashkin A, Dziedzic JM. 1987 Optical trapping and manipulation of viruses and bacteria. *Science* **235**, 1517–1520. (doi:10.1126/science.3547653)
3. De Vlaminck I, Dekker C. 2012 Recent advances in magnetic tweezers. *Annu. Rev. Biophys.* **41**, 453–472. (doi:10.1146/annurev-biophys-122311-100544)
4. Juan ML, Righini M, Quidant R. 2011 Plasmon nano-optical tweezers. *Nat. Photonics* **5**, 349–356. (doi:10.1038/nphoton.2011.56)
5. Meng L, Cai F, Li F, Zhou W, Niu L, Zheng H. 2019 Acoustic tweezers. *J. Phys. D: Appl. Phys.* **52**, 273001. (doi:10.1088/1361-6463/ab16b5)
6. Ashkin A, Dziedzic JM, Bjorkholm JE, Chu S. 2016 Observation of a single-beam gradient force optical trap for dielectric particles. In *Optical Angular Momentum*.
7. Neuman KC, Nagy A. 2008 Single-molecule force spectroscopy: optical tweezers, magnetic tweezers and atomic force microscopy. *Nat. Methods* **5**, 491–505. (doi:10.1038/nmeth.1218)
8. Ding X *et al.* 2013 Surface acoustic wave microfluidics. *Lab Chip* **13**, 3626–3649. (doi:10.1039/c3lc50361e)
9. Destgeer G, Sung HJ. 2015 Recent advances in microfluidic actuation and micro-object manipulation via surface acoustic waves. *Lab Chip* **15**, 2722–2728. (doi:10.1039/C5LC00265F)
10. Drinkwater BW. 2016 Dynamic-field devices for the ultrasonic manipulation of microparticles. *Lab Chip* **16**, 2360–2375. (doi:10.1039/C6LC00502K)
11. Wiklund M, Green R, Ohlin M. 2012 Acoustofluidics 14: applications of acoustic streaming in microfluidic devices. *Lab Chip* **12**, 2438–2451. (doi:10.1039/c2lc40203c)
12. Andrade MAB, Marzo A, Adamowski JC. 2020 Acoustic levitation in mid-air: recent advances, challenges, and future perspectives. *Appl. Phys. Lett.* **116**, 250501. (doi:10.1063/5.0012660)
13. Huang PH, Nama N, Mao Z, Li P, Rufo J, Chen Y, Xie Y, Wei CH, Wang L, Huang TJ. 2014 A reliable and programmable acoustofluidic pump powered by oscillating sharp-edge structures. *Lab Chip* **14**, 4319–4323. (doi:10.1039/C4LC00806E)
14. Kaynak M, Ozcelik A, Nourhani A, Lammert PE, Crespi VH, Huang TJ. 2017 Acoustic actuation of bioinspired microswimmers. *Lab Chip* **17**, 395–400. (doi:10.1039/C6LC01272H)
15. Ren L, Wang W, Mallouk TE. 2018 Two forces are better than one: combining chemical and acoustic propulsion for enhanced micromotor functionality. *Acc. Chem. Res.* **51**, 1948–1956. (doi:10.1021/acs.accounts.8b00248)
16. Ahmed D, Lu M, Nourhani A, Lammert PE, Stratton Z, Muddana HS, Crespi VH, Huang TJ. 2015 Selectively manipulable acoustic-powered microswimmers. *Sci. Rep.* **5**, 9744. (doi:10.1038/srep09744)
17. Dijkink RJ, Van Der Dennen JP, Ohl CD, Prosperetti A. 2006 The 'acoustic scallop': a bubble-powered actuator. *J. Micromech. Microeng.* **16**, 1653. (doi:10.1088/0960-1317/16/8/029)
18. Nelson BJ, Kaliakatsos IK, Abbott JJ. 2010 Microrobots for minimally invasive medicine. *Annu. Rev. Biomed. Eng.* **12**, 55–85. (doi:10.1146/annurev-bioeng-010510-103409)
19. Ceylan H, Giltinan J, Kozielski K, Sitti M. 2017 Mobile microrobots for bioengineering applications. *Lab Chip* **17**, 1705–1724. (doi:10.1039/C7LC00064B)
20. Dung Luong T, Trung Nguyen N. 2012 Surface acoustic wave driven microfluidics–a review. *Micro Nanosystemse* **2**, 217–225. (doi:10.2174/1876402911002030217)
21. Rao KJ, Li F, Meng L, Zheng H, Cai F, Wang W. 2015 A force to be reckoned with: a review of synthetic microswimmers powered by ultrasound. *Small* **11**, 2836–2846. (doi:10.1002/smll.201403621)
22. Muller PB, Barnkob R, Jensen MJH, Bruus H. 2012 A numerical study of microparticle acoustophoresis driven by acoustic radiation forces and streaming-induced drag forces. *Lab Chip* **12**, 4617–4627. (doi:10.1039/c2lc40612h)
23. Nama N, Huang PH, Huang TJ, Costanzo F. 2014 Investigation of acoustic streaming patterns around oscillating sharp edges. *Lab Chip* **14**, 2824–2836. (doi:10.1039/C4LC00191E)

24. Gor'kov LP. 2014 On the forces acting on a small particle in an acoustical field in an ideal fluid. In *Selected Papers of Lev P. Gor'kov*.
25. Guo F *et al.* 2016 Three-dimensional manipulation of single cells using surface acoustic waves. *Proc. Natl Acad. Sci. USA* **113**, 1522–1527. (doi:10.1073/pnas.1524813113)
26. Lei J. 2017 Formation of inverse Chladni patterns in liquids at microscale: roles of acoustic radiation and streaming-induced drag forces. *Microfluid. Nanofluid.* **21**, 50. (doi:10.1007/s10404-017-1888-5)
27. Ahmed D, Mao X, Shi J, Juluri BK, Huang TJ. 2009 A millisecond micromixer via single-bubble-based acoustic streaming. *Lab. Chip* **9**, 2738–2741. (doi:10.1039/b903687c)
28. Ahmed D, Baasch T, Jang B, Pane S, Dual J, Nelson BJ. 2016 Artificial swimmers propelled by acoustically activated flagella. *Nano Lett.* **16**, 4968–4974. (doi:10.1021/acs.nanolett.6b01601)
29. Leighton TG, Walton AJ, Pickworth MJ. 1990 Primary Bjerknes forces. *Eur. J. Phys.* **11**, 47–50. (doi:10.1088/0143-0807/11/1/009)
30. Marmottant P, Hilgenfeldt S. 2003 Controlled vesicle deformation and lysis by single oscillating bubbles. *Nature* **423**, 153–156. (doi:10.1038/nature01613)
31. Ochiai Y, Hoshi T, Rekimoto J. 2014 Three-dimensional mid-air acoustic manipulation by ultrasonic phased arrays. *PLoS ONE* **9**, e97590. (doi:10.1371/journal.pone.0097590)
32. Andrade MA, Ramos TS, Adamowski JC, Marzo A. 2020 Contactless pick-and-place of millimetric objects using inverted near-field acoustic levitation. *Appl. Phys. Lett.* **116**, 054104. (doi:10.1063/1.5138598)
33. Prisbrey M, Greenhall J, Guevara Vasquez F, Raeymaekers B. 2017 Ultrasound directed self-assembly of three-dimensional user-specified patterns of particles in a fluid medium. *J. Appl. Phys.* **121**, 014302. (doi:10.1063/1.4973190)
34. Watanabe A, Hasegawa K, Abe Y. 2018 Contactless fluid manipulation in air: droplet coalescence and active mixing by acoustic levitation. *Sci. Rep.* **8**, 10221. (doi:10.1038/s41598-018-28451-5)
35. Marzo A, Barnes A, Drinkwater BW. 2017 TinyLev: a multi-emitter single-axis acoustic levitator. *Rev. Sci. Instrum.* **88**, 085105. (doi:10.1063/1.4989995)
36. Marzo A, Drinkwater BW. 2019 Holographic acoustic tweezers. *Proc. Natl Acad. Sci. USA* **116**, 84–89. (doi:10.1073/pnas.1813047115)
37. Baresch D, Thomas JL, Marchiano R. 2016 Observation of a single-beam gradient force acoustical trap for elastic particles: acoustical tweezers. *Phys. Rev. Lett.* **116**, 024301. (doi:10.1103/PhysRevLett.116.024301)
38. Haake A, Dual J. 2005 Contactless micromanipulation of small particles by an ultrasound field excited by a vibrating body. *J. Acoust. Soc. Am.* **117**, 2752–2760. (doi:10.1121/1.1874592)
39. Courtney CR, Ong CK, Drinkwater BW, Bernassau AL, Wilcox PD, Cumming DR. 2012 Manipulation of particles in two dimensions using phase controllable ultrasonic standing waves. *Proc. R. Soc. A* **468**, 337–360. (doi:10.1098/rspa.2011.0269)
40. Seah S, Drinkwater B, Carter T, Malkin R, Subramanian S. 2014 Correspondence: dexterous ultrasonic levitation of millimeter-sized objects in air. *IEEE Trans. Ultrason. Ferroelectr. Freq. Control* **61**, 1233–1236. (doi:10.1109/TUFFC.2014.3022)
41. Marzo A, Seah SA, Drinkwater BW, Sahoo DR, Long B, Subramanian S. 2015 Holographic acoustic elements for manipulation of levitated objects. *Nat. Commun.* **6**, 8661. (doi:10.1038/ncomms9661)
42. Zhang R, Guo H, Deng W, Huang X, Li F, Lu J, Liu Z. 2020 Acoustic tweezers and motor for living cells. *Appl. Phys. Lett.* **116**, 1–5. (doi:10.1063/5.0002327)
43. Jiménez-Gambín S, Jiménez N, Benlloch JM, Camarena F. 2019 Generating Bessel beams with broad depth-of-field by using phase-only acoustic holograms. *Sci. Rep.* **9**, 20104. (doi:10.1038/s41598-019-56369-z)
44. Franklin A, Marzo A, Malkin R, Drinkwater BW. 2017 Three-dimensional ultrasonic trapping of micro-particles in water with a simple and compact two-element transducer. *Appl. Phys. Lett.* **111**, 094101. (doi:10.1063/1.4992092)
45. Nakahara J, Yang B, Smith JR. 2020 Contact-less manipulation of millimeter-scale objects via ultrasonic levitation. *IEEE RAS/EMBS International Conference on Biomedical Robotics and Biomechatronics*.
46. Tian Z *et al.* 2019 Wave number–spiral acoustic tweezers for dynamic and reconfigurable manipulation of particles and cells. *Sci. Adv.* **5**, eaau6062. (doi:10.1126/sciadv.aau6062)

47. Kang P *et al.* 2020 Acoustic tweezers based on circular, slanted-finger interdigital transducers for dynamic manipulation of micro-objects. *Lab Chip* **20**, 987–994. (doi:10.1039/C9LC01124B)
48. Zhang P *et al.* 2019 Contactless, programmable acoustofluidic manipulation of objects on water. *Lab Chip* **19**, 3397–3404. (doi:10.1039/C9LC00465C)
49. Courtney CR, Drinkwater BW, Demore CE, Cochran S, Grinenko A, Wilcox PD. 2013 Dexterous manipulation of microparticles using Bessel-function acoustic pressure fields. *Appl. Phys. Lett.* **102**, 123508. (doi:10.1063/1.4798584)
50. Baudoin M, Gerbedoen JC, Riaud A, Matar OB, Smagin N, Thomas JL. 2019 Folding a focalized acoustical vortex on a flat holographic transducer: miniaturized selective acoustical tweezers. *Sci. Adv.* **5**, eaav1967. (doi:10.1126/sciadv.aav1967)
51. Zhang SP *et al.* 2018 Digital acoustofluidics enables contactless and programmable liquid handling. *Nat. Commun.* **9**, 2928. (doi:10.1038/s41467-018-05297-z)
52. Latifi K, Kopitca A, Zhou Q. 2020 Model-free control for dynamic-field acoustic manipulation using reinforcement learning. *IEEE Access* **8**, 20 597–20 606. (doi:10.1109/ACCESS.2020.2969277)
53. Shi J, Huang H, Stratton Z, Huang Y, Huang TJ. 2009 Continuous particle separation in a microfluidic channel via standing surface acoustic waves (SSAW). *Lab Chip* **9**, 3354–3359. (doi:10.1039/b915113c)
54. Destgeer G, Jung JH, Park J, Ahmed H, Park K, Ahmad R, Sung HJ. 2017 Acoustic impedance-based manipulation of elastic microspheres using travelling surface acoustic waves. *RSC Adv.* **7**, 22 524–22 530. (doi:10.1039/C7RA01168G)
55. Collins DJ, Ma Z, Han J, Ai Y. 2017 Continuous micro-vortex-based nanoparticle manipulation via focused surface acoustic waves. *Lab Chip* **17**, 91–103. (doi:10.1039/C6LC01142J)
56. Connacher W, Zhang N, Huang A, Mei J, Zhang S, Gopesh T, Friend J. 2018 Micro/nano acoustofluidics: Materials, phenomena, design, devices, and applications. *Lab Chip* **18**, 1952–1996. (doi:10.1039/C8LC00112J)
57. Shi J, Ahmed D, Mao X, Lin SCS, Lawit A, Huang TJ. 2009 Acoustic tweezers: Patterning cells and microparticles using standing surface acoustic waves (SSAW). *Lab Chip* **9**, 2890–2895. (doi:10.1039/b910595f)
58. Nam J, Lim H, Kim C, Yoon Kang J, Shin S. 2012 Density-dependent separation of encapsulated cells in a microfluidic channel by using a standing surface acoustic wave. *Biomicrofluidics* **6**, 024120. (doi:10.1063/1.4718719)
59. Ahmed H, Destgeer G, Park J, Afzal M, Sung HJ. 2018 Sheathless focusing and separation of microparticles using tilted-angle traveling surface acoustic waves. *Anal. Chem.* **90**, 8546–8552. (doi:10.1021/acs.analchem.8b01593)
60. Li S, Guo F, Chen Y, Ding X, Li P, Wang L, Cameron CE, Huang TJ. 2014 Standing surface acoustic wave based cell coculture. *Anal. Chem.* **86**, 9853–9859. (doi:10.1021/ac502453z)
61. Franke T, Abate AR, Weitz DA, Wixforth A. 2009 Surface acoustic wave (SAW) directed droplet flow in microfluidics for PDMS devices. *Lab Chip* **9**, 2625–2627. (doi:10.1039/b906819h)
62. Schmid L, Franke T. 2018 Real-time size modulation and synchronization of a microfluidic dropmaker with pulsed surface acoustic waves (SAW). *Sci. Rep.* **8**, 1–7. (doi:10.1038/s41598-018-22529-w)
63. Evander M, Gidlöf O, Olde B, Erlinge D, Laurell T. 2015 Non-contact acoustic capture of microparticles from small plasma volumes. *Lab Chip* **15**, 2588–2596. (doi:10.1039/C5LC00290G)
64. Wu M *et al.* 2017 Isolation of exosomes from whole blood by integrating acoustics and microfluidics. *Proc. Natl Acad. Sci. USA* **114**, 10 584–10 589. (doi:10.1073/pnas.1709210114)
65. Wang K, Zhou W, Lin Z, Cai F, Li F, Wu J, Meng L, Niu L, Zheng H. 2018 Sorting of tumour cells in a microfluidic device by multi-stage surface acoustic waves. *Sensors Actuators, B: Chem.* **258**, 1174–1183. (doi:10.1016/j.snb.2017.12.013)
66. Olm F, Urbansky A, Dykes JH, Laurell T, Scheding S. 2019 Label-free neuroblastoma cell separation from hematopoietic progenitor cell products using acoustophoresis - towards cell processing of complex biological samples. *Sci. Rep.* **9**, 1–11. (doi:10.1038/s41598-018-37186-2)
67. Urbansky A, Olm F, Scheding S, Laurell T, Lenshof A. 2019 Label-free separation of leukocyte subpopulations using high throughput multiplex acoustophoresis. *Lab Chip* **19**, 1406–1416. (doi:10.1039/C9LC00181F)

68. Ota N, Yalikun Y, Suzuki T, Lee SW, Hosokawa Y, Goda K, Tanaka Y. 2019 Enhancement in acoustic focusing of micro and nanoparticles by thinning a microfluidic device. *R. Soc. Open Sci.* **6**, 181776. (doi:10.1098/rsos.181776)
69. Zhang J *et al.* 2019 Surface acoustic waves enable rotational manipulation of Caenorhabditis elegans. *Lab Chip* **19**, 984–992. (doi:10.1039/C8LC01012A)
70. Zhang J, Hartman JH, Chen C, Yang S, Li Q. 2020 Fluorescence-based sorting of Caenorhabditis. *Lab Chip* **20**, 1729–1739. (doi:10.1039/D0LC00051E)
71. Van Assche D, Reithuber E, Qiu W, Laurell T, Henriques-Normark B, Mellroth P, Ohlsson P, Augustsson P. 2020 Gradient acoustic focusing of sub-micron particles for separation of bacteria from blood lysate. *Sci. Rep.* **10**, 3670. (doi:10.1038/s41598-020-60338-2)
72. Zhao S *et al.* 2020 A disposable acoustofluidic chip for nano/microparticle separation using unidirectional acoustic transducers. *Lab. Chip* **20**, 1298–1308. (doi:10.1039/D0LC00106F)
73. Li P, Liang M, Lu X, Chow JJM, Ramachandra CJ, Ai Y. 2019 Sheathless acoustic fluorescence activated cell sorting (aFACS) with high cell viability. *Anal. Chem.* **91**, 15 425–15 435. (doi:10.1021/acs.analchem.9b03021)
74. Wu M, Ozcelik A, Rufo J, Wang Z, Fang R, Jun Huang T. 2019 Acoustofluidic separation of cells and particles. *Microsyst. Nanoeng.* **5**, 32. (doi:10.1038/s41378-019-0064-3)
75. Collins DJ, Khoo BL, Ma Z, Winkler A, Weser R, Schmidt H, Han J, Ai Y. 2017a Selective particle and cell capture in a continuous flow using micro-vortex acoustic streaming. *Lab Chip* **17**, 1769–1777. (doi:10.1039/C7LC00215G)
76. Collins DJ, Ma Z, Han J, Ai Y. 2017b Continuous micro-vortex-based nanoparticle manipulation via focused surface acoustic waves. *Lab Chip* **17**, 91–103. (doi:10.1039/C6LC01142J)
77. Lu X, Soto F, Li J, Li T, Liang Y, Wang J. 2017 Topographical manipulation of microparticles and cells with acoustic microstreaming. *ACS Appl. Mater. Interfaces* **9**, 38870. (doi:10.1021/acsami.7b15237)
78. Ozcelik A, Nama N, Huang PH, Kaynak M, McReynolds MR, Hanna-Rose W, Huang TJ. 2016 Acoustofluidic rotational manipulation of cells and organisms using oscillating solid structures. *Small (Weinheim an der Bergstrasse, Germany)* **12**, 5120–5125. (doi:10.1002/smll.201601760)
79. Ahmed D, Ozcelik A, Bojanala N, Nama N, Upadhyay A, Chen Y, Hanna-Rose W, Huang TJ. 2016 Rotational manipulation of single cells and organisms using acoustic waves. *Nat. Commun.* **7**, 1–11. (doi:10.1038/ncomms11085)
80. Läubli N, Shamsudhin N, Ahmed D, Nelson BJ. 2017 Controlled three-dimensional rotation of single cells using acoustic waves. *Procedia CIRP* **65**, 93–98. (doi:10.1016/j.procir.2017.04.028)
81. Bachman H, Chen C, Rufo J, Zhao S, Yang S, Tian Z, Nama N, Huang PH, Huang TJ. 2020 An acoustofluidic device for efficient mixing over a wide range of flow rates. *Lab Chip* **20**, 1238–1248. (doi:10.1039/C9LC01171D)
82. Wu Z, Cai H, Ao Z, Nunez A, Liu H, Bondesson M, Guo S, Guo F. 2019 A digital acoustofluidic pump powered by localized fluid-substrate interactions. *Anal. Chem.* **91**, 7097–7103. (doi:10.1021/acs.analchem.9b00069)
83. Gao Y, Wu M, Lin Y, Zhao W, Xu J. 2020 Acoustic bubble-based bidirectional micropump. *Microfluid. Nanofluid.* **24**, 29. (doi:10.1007/s10404-020-02334-6)
84. Patel MV, Nanayakkara IA, Simon MG, Lee AP. 2014 Cavity-induced microstreaming for simultaneous on-chip pumping and size-based separation of cells and particles. *Lab Chip* **14**, 3860. (doi:10.1039/C4LC00447G)
85. Garg N, Westerhof TM, Liu V, Liu R, Nelson EL, Lee AP. 2018 Whole-blood sorting, enrichment and in situ immunolabeling of cellular subsets using acoustic microstreaming. *Microsyst. Nanoeng.* **4**, 17085. (doi:10.1038/micronano.2017.85)
86. Zhao S *et al.* 2019 On-chip stool liquefaction via acoustofluidics. *Lab Chip* **19**, 941–947. (doi:10.1039/C8LC01310A)
87. Feng L, Song B, Zhang D, Jiang Y, Arai F. 2018 On-chip tunable cell rotation using acoustically oscillating asymmetrical microstructures. *Micromachines* **9**, 596. (doi:10.3390/mi9110596)
88. Mohanty S, Siciliani de Cumis U, Solsona M, Misra S. 2019 Bi-directional transportation of micro-agents induced by symmetry-broken acoustic streaming. *AIP Adv.* **9**, 035352. (doi:10.1063/1.5089717)

89. Kaynak M, Ozcelik A, Nama N, Nourhani A, Lammert PE, Crespi VH, Huang TJ. 2016 Acoustofluidic actuation of in situ fabricated microrotors. *Lab Chip* **16**, 3532–3537. (doi:10.1039/C6LC00443A)
90. Saito M, Kasai Y, Kumon H, Sakuma S, Arai F. 2020 High-Speed and High-Resolution On-Chip Pumping Utilizing Asymmetric Flow Resistors. In *Proc. of the IEEE Int. Conf. on Micro Electro Mechanical Systems (MEMS)*.
91. Kaynak M, Ayhan F, Sakar MS. 2019 Compound micromachines powered by acoustic streaming. In *Proc. - IEEE Int. Conf. on Robotics and Automation*.
92. Vasileiou T, Foresti D, Bayram A, Poulikakos D, Ferrari A. 2016 Toward contactless biology: acoustophoretic DNA transfection. *Sci. Rep.* **6**, 20023. (doi:10.1038/srep20023)
93. Cao HL, Yin DC, Guo YZ, Ma XL, He J, Guo WH, Xie XZ, Zhou BR. 2012 Rapid crystallization from acoustically levitated droplets. *J. Acoust. Soc. Am.* **131**, 3164–3172. (doi:10.1121/1.3688494)
94. O'Rorke R, Winkler A, Collins D, Ai Y. 2020 Slowness curve surface acoustic wave transducers for optimized acoustic streaming. *RSC Adv.* **10**, 11 582–11 589. (doi:10.1039/C9RA10452F)
95. Wang W, Castro LA, Hoyos M, Mallouk TE. 2012 Autonomous motion of metallic microrods propelled by ultrasound. *ACS Nano* **6**, 6122–6132. (doi:10.1021/nn301312z)
96. Wang W, Li S, Mair L, Ahmed S, Huang TJ, Mallouk TE. 2014 Acoustic propulsion of nanorod motors inside living cells. *Angewandte Chemie - Int. Ed.* **53**, 3201–3204. (doi:10.1002/anie.201309629)
97. Ahmed S, Wang W, Bai L, Gentekos DT, Hoyos M, Mallouk TE. 2016 Density and shape effects in the acoustic propulsion of bimetallic nanorod motors. *ACS Nano* **10**, 4763–4769. (doi:10.1021/acsnano.6b01344)
98. Sabrina S, Tasinkevych M, Ahmed S, Brooks AM, Olvera De La Cruz M, Mallouk TE, Bishop KJ. 2018 Shape-directed microspinners powered by ultrasound. *ACS Nano* **12**, 2939–2947. (doi:10.1021/acsnano.8b00525)
99. Esteban-Fernández De Ávila B, Martín A, Soto F, Lopez-Ramirez MA, Campuzano S, Vásquez-Machado GM, Gao W, Zhang L, Wang J. 2015 Single cell real-time miRNAs sensing based on nanomotors. *ACS Nano* **9**, 6756–6764. (doi:10.1021/acsnano.5b02807)
100. Esteban-Fernández De Ávila B, Ramírez-Herrera DE, Campuzano S, Angsantikul P, Zhang L, Wang J. 2017 Nanomotor-Enabled pH-Responsive intracellular delivery of caspase-3: toward rapid cell apoptosis. *ACS Nano* **11**, 5367–5374. (doi:10.1021/acsnano.7b01926)
101. De Ávila BEF, Angsantikul P, Ramírez-Herrera DE, Soto F, Teymourian H, Dehaini D, Chen Y, Zhang L, Wang J. 2018 Hybrid biomembrane-functionalized nanorobots for concurrent removal of pathogenic bacteria and toxins. *Sci. Rob.* **3**, eaat0485. (doi:10.1126/scirobotics.aat0485)
102. Nadal F, Lauga E. 2014 Asymmetric steady streaming as a mechanism for acoustic propulsion of rigid bodies. *Phys. Fluids* **26**, 082001. (doi:10.1063/1.4891446)
103. Collis JF, Chakraborty D, Sader JE. 2017 Autonomous propulsion of nanorods trapped in an acoustic field. *J. Fluid Mech.* **825**, 29–48. (doi:10.1017/jfm.2017.381)
104. Liu J, Ruan H. 2020 Modeling of an acoustically actuated artificial micro-swimmer. *Bioinspir. Biomim.* **15**, 036002. (doi:10.1088/1748-3190/ab6a61)
105. Feng J, Yuan J, Cho SK. 2016 2-D steering and propelling of acoustic bubble-powered microswimmers. *Lab Chip* **16**, 2317–2325. (doi:10.1039/C6LC00431H)
106. Chen Q, Liu FW, Xiao Z, Sharma N, Cho SK, Kim K. 2019 Ultrasound tracking of the acoustically actuated microswimmer. *IEEE Trans. Biomed. Eng.* **66**, 3231–3237. (doi:10.1109/TBME.2019.2902523)
107. Liu FW, Cho SK. 2019 3-D Micro swimming drone with maneuverability. In *Proc. of the IEEE Int. Conf. on Micro Electro Mechanical Systems (MEMS)*.
108. Jang D, Jeon J, Chung SK. 2018 Acoustic bubble-powered miniature rotor for wireless energy harvesting in a liquid medium. *Sensors Actuators, A Phys.* **276**, 296–303. (doi:10.1016/j.sna.2018.04.023)
109. Youssefi O, Diller E. 2019 Contactless robotic micromanipulation in air using a magneto-acoustic system. *IEEE Rob. Autom. Lett.* **4**, 1580–1586. (doi:10.1109/LRA.2019.2896444)
110. Garcia-Gradilla V *et al.* 2013 Functionalized ultrasound-propelled magnetically guided nanomotors: toward practical biomedical applications. *ACS Nano* **7**, 9232–9240. (doi:10.1021/nn403851v)

111. Ahmed S, Wang W, Mair LO, Fraleigh RD, Li S, Castro LA, Hoyos M, Huang TJ, Mallouk TE. 2013 Steering acoustically propelled nanowire motors toward cells in a biologically compatible environment using magnetic fields. *Langmuir* **29**, 16 113–16 118. (doi:10.1021/la403946j)
112. Soto F, Wagner GL, Garcia-Gradilla V, Gillespie KT, Lakshmipathy DR, Karshalev E, Angell C, Chen Y, Wang J. 2016 Acoustically propelled nanoshells. *Nanoscale* **8**, 17 788–17 793. (doi:10.1039/C6NR06603H)
113. Ahmed D, Dillinger C, Hong A, Nelson BJ. 2017 Artificial acousto-magnetic soft microswimmers. *Adv. Mater. Technol.* **2**, 1700050. (doi:10.1002/admt.201700050)
114. Ren L, Nama N, McNeill JM, Soto F, Yan Z, Liu W, Wang W, Wang J, Mallouk TE. 2019 3D steerable, acoustically powered microswimmers for single-particle manipulation. *Sci. Adv.* **5**, eaax3084. (doi:10.1126/sciadv.aax3084)
115. Aghakhani A, Yasa O, Wrede P, Sitti M. 2020 Acoustically powered surface-slipping mobile microrobots. *Proc. Natl Acad. Sci. USA* **117**, 3469–3477. (doi:10.1073/pnas.1920099117)
116. Jeong J, Jang D, Kim D, Lee D, Chung SK. 2020 Acoustic bubble-based drug manipulation: carrying, releasing and penetrating for targeted drug delivery using an electromagnetically actuated microrobot. *Sensors Actuators A Phys.* **306**, 111973. (doi:10.1016/j.sna.2020.111973)
117. Wu Z *et al.* 2014 Turning erythrocytes into functional micromotors. *ACS Nano* **8**, 12 041–12 048. (doi:10.1021/nn506200x)
118. Ahmed D, Baasch T, Blondel N, Läubli N, Dual J, Nelson BJ. 2017 Neutrophil-inspired propulsion in a combined acoustic and magnetic field. *Nat. Commun.* **8**, 1–8. (doi:10.1038/s41467-016-0009-6)
119. Kagan D, Benchimol MJ, Claussen JC, Chuluun-Erdene E, Esener S, Wang J. 2012 Acoustic droplet vaporization and propulsion of perfluorocarbon-loaded microbullets for targeted tissue penetration and deformation. *Angewandte Chemie - Int. Ed.* **51**, 7519–7522. (doi:10.1002/anie.201201902)
120. Soto F, Martin A, Ibsen S, Vaidyanathan M, Garcia-Gradilla V, Levin Y, Escarpa A, Esener SC, Wang J. 2016 Acoustic microcannons: toward advanced microballistics. *ACS Nano* **10**, 1522–1528. (doi:10.1021/acsnano.5b07080)
121. Wang W, Duan W, Zhang Z, Sun M, Sen A, Mallouk TE. 2015 A tale of two forces: simultaneous chemical and acoustic propulsion of bimetallic micromotors. *Chem. Commun.* **51**, 1020–1023. (doi:10.1039/C4CC09149C)
122. Xu T, Soto F, Gao W, Dong R, Garcia-Gradilla V, Magaña E, Zhang X, Wang J. 2015 Reversible swarming and separation of self-propelled chemically powered nanomotors under acoustic fields. *J. Am. Chem. Soc.* **137**, 2163–2166. (doi:10.1021/ja511012v)
123. Ren L, Zhou D, Mao Z, Xu P, Huang TJ, Mallouk TE. 2017 Rheotaxis of bimetallic micromotors driven by chemical-acoustic hybrid power. *ACS Nano* **11**, 10 591–10 598. (doi:10.1021/acsnano.7b06107)
124. Louf JF, Bertin N, Dollet B, Stephan O, Marmottant P. 2018 Hovering microswimmers exhibit ultrafast motion to navigate under acoustic forces. *Adv. Mater. Interfaces* **5**, 1800425. (doi:10.1002/admi.201800425)
125. van Neer P, Volker A, Berkhoff A, Schrama T, Akkerman H, van Breemen A, Peeters L, van der Steen JL, Gelinck G. 2019 Development of a flexible large-area array based on printed polymer transducers for mid-air haptic feedback. In *2019 Int. Congress on Ultrasonics*.
126. Memoli G, Caleap M, Asakawa M, Sahoo DR, Drinkwater BW, Subramanian S. 2017 Metamaterial bricks and quantization of meta-surfaces. *Nat. Commun.* **8**, 14608. (doi:10.1038/ncomms14608)
127. Prat-Camps J, Christopoulos G, Hardwick J, Subramanian S. 2020 A manually reconfigurable reflective spatial sound modulator for ultrasonic waves in air. *Adv. Mater. Technol.* **5**, 2000041. (doi:10.1002/admt.202000041)
128. Raymond SJ, Collins DJ, O'Rorke R, Tayebi M, Ai Y, Williams J. 2020 A deep learning approach for designed diffraction-based acoustic patterning in microchannels. *Sci. Rep.* **10**, 1–12. (doi:10.1038/s41598-020-65453-8)
129. Zhou H, Niu L, Xia X, Lin Z, Liu X, Su M, Guo R, Meng L, Zheng H. 2019 Wearable ultrasound improves motor function in an MPTP mouse model of Parkinson's disease. *IEEE Trans. Biomed. Eng.* **66**, 3006–3013. (doi:10.1109/TBME.2019.2899631)
130. McNeill JM, Nama N, Braxton JM, Mallouk TE. 2020 Wafer-scale fabrication of micro- to nanoscale bubble swimmers and their fast autonomous propulsion by ultrasound. *ACS Nano* **14**, 7520–7528. (doi:10.1021/acsnano.0c03311)

131. Gao C, Lin Z, Zhou C, Wang D, He Q. 2020 Acoustophoretic motion of erythrocyte–mimicking hemoglobin micromotors. *Chin. J. Chem.* **38**, 1589–1594. (doi:10.1002/cjoc.202000347)
132. Zhou Y. 2015 Application of acoustic droplet vaporization in ultrasound therapy. *J. Ther. Ultrasound* **3**, 1–18. (doi:10.1186/s40349-015-0041-8)
133. Baresch D, Garbin V. 2020 Acoustic trapping of microbubbles in complex environments and controlled payload release. *Proc. Natl Acad. Sci. USA* **117**, 15 490–15 496. (doi:10.1073/pnas.2003569117)
134. Ongaro F, Niehoff D, Mohanty S, Misra S. 2019 A contactless and biocompatible approach for 3D active microrobotic targeted drug delivery. *Micromachines* **10**, 504. (doi:10.3390/mi10080504)
135. Ahmed D, Hauri D, Sukhov A, Rodrigue D, Gian M, Harting J, Nelson B. 2020 Bio-inspired acousto-magnetic microswarm robots with upstream motility. (http://arxiv.org/abs/2005.12703).
136. Lu X, Soto F, Li J, Li T, Liang Y, Wang J. 2017 Topographical manipulation of microparticles and cells with acoustic microstreaming. *ACS Appl. Mater. Interfaces* **9**, 38 870–38 876. (doi:10.1021/acsami.7b15237)
137. Ghanem MA, Maxwell AD, Wang YN, Cunitz BW, Khokhlova VA, Sapozhnikov OA, Bailey MR. 2020 Noninvasive manipulation of objects in a living body. *Proc. Natl Acad. Sci. USA* **117**, 16 848–16 855. (doi:10.1073/pnas.2001779117)
138. Xie Y, Shen C, Wang W, Li J, Suo D, Popa BI, Jing Y, Cummer SA. 2016 Acoustic holographic rendering with two-dimensional metamaterial-based passive phased array. *Sci. Rep.* **6**, 35437. (doi:10.1038/srep35437)
139. Xie H, Sun M, Fan X, Lin Z, Chen W, Wang L, Dong L, He Q. 2019 Reconfigurable magnetic microrobot swarm: multimode transformation, locomotion, and manipulation. *Sci. Rob.* **4**, eaav8006. (doi:10.1126/scirobotics.aav8006)
140. Qiu T, Adams F, Palagi S, Melde K, Mark A, Wetterauer U, Miernik A, Fischer P. 2017 Wireless acoustic-surface actuators for miniaturized endoscopes. *ACS Appl. Mater. Interfaces* **9**, 42 536–42 543. (doi:10.1021/acsami.7b12755)